Inbreeding depression depends on the body size and environmental conditions in a threatened songbird, the aquatic warbler *Acrocephalus paludicola*

Justyna Kubacka[1], Larissa Souza Arantes[2,3], Magdalena Herdegen-Radwan[4], Tomasz S. Osiejuk[4], Sarah Sparmann[2,5] and Camila Mazzoni[2,3]

[1] Museum and Institute of Zoology of the Polish Academy of Sciences, Wilcza 64, 00-679 Warszawa, Poland

[2] Berlin Center for Genomics in Biodiversity Research, Königin-Luise-Straße 6-8, 14195 Berlin, Germany

[3] Leibniz Institute for Zoo and Wildlife Research, Alfred-Kowalke-Straße 17, 10315 Berlin, Germany

[4] Department of Behavioural Ecology, Faculty of Biology, Adam Mickiewicz University, Uniwersytetu Poznańskiego 6, 61-614 Poznań, Poland

[5] Leibniz Institute of Freshwater Ecology and Inland Fisheries, Müggelseedamm 310, 12587 Berlin Berlin, Germany

[*] corresponding author, e-mail: jkubacka@miiz.waw.pl

ORCIDs:

Justyna Kubacka 0000-0003-1211-8324

Larissa Souza Arantes 0000-0003-1374-6701

Magdalena Herdegen-Radwan 0000-0001-6593-3256

Tomasz S. Osiejuk 0000-0001-5980-7421

Camila Mazzoni 0000-0001-6758-5427

Sarah Sparmann 0000-0001-9278-4081

Abstract

While inbreeding is known to affect individual fitness and thus extinction risk in populations, studies have under-represented non-model species of conservation concern and rarely sought conditionality of inbreeding depression. Here, using SNPs identified with RAD-seq, we determined inbreeding depression in a threatened passerine, the aquatic warbler *Acrocephalus paludicola*, and whether its magnitude depends on phenotypic and environmental factors. We found no support for an association of the inbreeding coefficient (*F*) with the long-term return rate to breeding grounds and seasonal breeding success in adult males, and with the clutch size, hatch failures, nestling mortality, and fledged brood size in adult females. However, the *F* of adults with small tarsi (a proxy for structural body size) was negatively associated with the seasonal breeding success (in males) and clutch size (in females). We found no support for a relationship between nestling or parental *F* and nestling scaled-mass index (SMI) on days 2, 5 and 9 post-hatch. Nestling tarsus was negatively related to father *F* on days 5 and 9, and less strongly to mother *F* on day 5, but not to nestling *F*. The mother *F* effects on nestling tarsus and SMI were more negative in higher temperatures and the father *F* was more negatively related to nestling tarsus on later laying dates. The nestling *F* was more negatively associated with SMI under lower temperatures and rainfall. Neither the parental, nor the chick *F* effects on tarsus and SMI were found to interact with nestling sex, brood size and prey abundance. The inbreeding load on the adult male long-term survival rates was low for the mean covariates under study, but the decrease in fitness in the most inbred individuals, relative to the least inbred ones was high (~76%) for the breeding success in small-tarsus males and moderate (~10%) for the clutch size in small-tarsus females. We conclude that in the aquatic warbler (1) while inbreeding depression for the average phenotypic and environmental variables studied is not supported, (2) it is moderate to strong in small-bodied adults, (3) for chick condition, it depends on the weather, and (4) parental inbreeding effects could carry over to the next generation.

Introduction

Inbreeding results from mating between kin, non-random mating or division of a population into isolated groups (Keller & Waller 2002). It leads to increased genomic homozygosity and accumulation of harmful mutations, which are typically recessive and thus more often expressed in highly homozygous, inbred individuals. Consequently, more inbred individuals have compromised fitness. Inbreeding depression, which is decrease in fitness with increase in inbreeding, has been found across plant and animal taxa (Ralls *et al.* 1988, Keller & Waller 2002) and is especially strong in wild populations (Crnokrak & Roff 1999). Inbreeding affects a range of important fitness components. For instance, in wild-ranging animal species, it negatively affects sperm quality (Gage *et al.* 2006, Hinkson & Poo 2020), embryo development (Noordwijk & Scharloo 1981, Kruuk *et al.* 2002, Hemmings *et al.* 2012a), juvenile survival (Kruuk *et al.* 2002, Kennedy *et al.* 2014), annual reproductive success (Huisman *et al.* 2016, Niskanen *et al.* 2020) and the lifetime reproductive success (Grueber *et al.* 2010, Huisman *et al.* 2016, Harrisson *et al.* 2019). As a consequence, inbreeding depression decreases population viability and contributes to extinction risk (Westemeier *et al.* 1998, Brook *et al.* 2002, O'Grady *et al.* 2006, Nonaka *et al.* 2019). Therefore, evaluating its impact is of particular importance in populations of conservation concern.

Inbreeding depression is expected to be more pronounced in harsher environments or individuals of lower condition (Armbruster & Reed 2005). For example, low food availability and high number of competitors increased the magnitude of inbreeding depression on survival in an island population of Darwin's finches (Keller *et al.* 2002). A long-term study on the great tit (*Parus major*) found that inbreeding by environment interactions, while generally weak, were more marked in adverse conditions that are more closely related to fitness (Szulkin & Sheldon 2007). Laboratory experiments on insects showed that inbreeding effects on offspring survival increased with mother age (Fox & Reed 2010) and environmental toxicity (Nowak *et al.* 2007). However, evaluation of the conditionality of inbreeding depression in wild populations has not been frequent, while determining its magnitude across individual traits and environmental conditions would yield more accurate inbreeding depression estimates, especially in threatened populations.

Here, we determined the strength of inbreeding depression on fitness-related traits in an IUCN-threatened songbird, the aquatic warbler *Acrocephalus paludicola*. The aquatic warbler is a habitat specialist that breeds mainly in open, mesotrophic and permanently wet fen mires (Tanneberger *et al.* 2018b). It is a long-distance migrant wintering in sub-Saharan Western Africa (Le Nevé *et al.* 2018, Tanneberger *et al.* 2018b). Following the gradual disappearance of fens, which accelerated especially over the past 100-200 years due to peat extraction, changes in hydrological regime, drainage, eutrophication and succession, the extent of occurrence of the aquatic warbler shrank considerably (Tanneberger *et al.* 2018a). This led to a steep decline in the population size, amounting to 95% only between 1950-80, and its extinction from western Europe by the end of the

20th century (Briedis & Keišs 2016, Flade et al. 2018). Today, the breeding range of the aquatic warbler is constrained to east-central Europe, which holds c. 98% of the total population estimated at 12200 singing males (Flade *et al.* 2018). A recent study demonstrated that genetic diversity in the aquatic warbler is low and comparable to that of other threatened bird species (Evans & Sheldon 2008, Vitorino *et al.* 2019, Kubacka *et al.* 2023). As it is habitat specialists that are more strongly affected by loss of genetic diversity due to habitat loss and fragmentation (Matthews *et al.* 2014, Pflüger *et al.* 2019), to improve prediction of extinction risk and to tailor conservation actions for the aquatic warbler, it is therefore important to determine the magnitude of inbreeding depression in this species.

Specifically, we aimed at 1) estimating inbreeding depression by relating adult inbreeding rates to adult reproductive success and survival traits, and relating parental and nestling inbreeding rates to nestling body size and condition; 2) evaluating whether the inbreeding depression in the aquatic warbler is conditioned by phenotypic variables corresponding to individual quality, and by environmental variables that are expected to affect fecundity, offspring development and survival; and 3) assessing the inbreeding load and change in fitness associated with inbreeding.

Methods

Study area and sampling

The study was conducted between May and August of 2017-2023, in the Biebrza Valley (Poland), which holds about 25% (c. 2,700 singing males) of the global breeding population of the aquatic warbler. The habitat is permanently water-logged open fen mire and to a less extent wet meadows, all dominated by sedges *Carex* spp. Three study areas were used, referred to as Ławki (N 53º17’11.4’’, E 22º33’49.2’’), Szorce (N 53º17’34.8’’, E 22º37’15.9’’) and Mścichy (53º25’41.7’’ E 22º30’17.0’’). Each study area consisted of two 10-20-hectare (ha) study plots, totalling 70 ha over all the study areas. The male densities in Ławki and Szorce were comparable, while Mścichy had male densities lower than in the other two study areas.

Between 2017-2019 we conducted nest search, bird capture and blood-sampling. Adult males were caught with mist-nets and marked with unique metal and colour rings. They were blood-sampled through puncture of the brachial vein with a sterile needle and collecting approx. 10-120 ul of blood with a capillary. We measured tarsus length (by measuring the distance from the notch on the metatarsus to the top of the bone above the folded toes, with a calliper to the nearest 0.1 mm), wing length (with a ruler to the nearest mm) and body mass (with an electronic Kern CM 150-1N balance to the nearest 0.1 g). Nests were located by search and observation of alarming females every 2-7 days in each plot (Kubacka *et al.* 2014), with a three-week break between the two breeding peaks. We made all efforts to find most nests within the study plots. Tarsus and body mass

of the chicks were measured, as above, on days 2, 5 and 9 post-hatch for chicks in nests found at the egg stage or day 1-2 post-hatch (assuming day 0 as the day when most eggs in a nest were hatched). Chicks were blood-sampled on day 9 post-hatch through brachial venepuncture, as above. Nests were monitored every 1-5 days from the finding day, to determine number of fledged young and nest fate. Females were mist-netted by the nest and blood-sampled as above. We collected approx. 10-80 and 10-120 µl blood from a chick and a female, respectively. Each blood sample was immediately placed in a vial with an o-ring seal, containing 2 ml of 96% EtOH, and shaken to avoid formation of large clots. In total, we blood-sampled 174 males, 321 chicks from 71 nests and 105 mothers.

Between May-July 2018-2023, we systematically searched the study plots and their surroundings up to 150 m off border for colour-ringed adult individuals. The search effort was 0.15-0.92 person-days per hectare. The colour-ring code was read with an 80-mm-lens and 20-60 magnification scope. The position of each resighted individual was stored in a GPS receiver. In addition, we searched for recoveries of the ringed individuals (mostly during migration) in the Polish Bird Ringing Database (POLRING). These recoveries, as well as retraps of colour-ringed individuals in the study areas between 2018-2023 were included as resights to calculate return rate (see below).

We obtained the following weather data from the Polish Institute of Meteorology and Water Management (IMGW) : daily sum of rainfall in mm, daily minimum ground temperature and daily maximum temperature, all between May 1 and August 31 in the years 2017-2019.

We sampled arthropod prey within about 30 m from the nest, by sweep-netting at the pace of approx. 1 sweep per 1 second, starting 3 m from the nest and walking 50 steps away from the nest. Sweep-netting was conducted on three such transects around each nest, oriented radially. All the arthropod prey caught in the sweep-net was placed in a plastic bag and frozen upon arrival from the field. The arthropods were determined to the order level and the count of individuals per each taxonomic group per nest was determined.

Molecular marker detection and genotyping

DNA was isolated with the Xpure™ Blood Mini kit (cat. no. 097-50-M1, A&A Biotechnology, Poland). 200-300 ul of blood suspended in 96% EtOH were used per individual and the proteinase K digestion time was two-three hours. The remaining steps were performed according to the manufacturer's protocol.

To determine inbreeding rates, we used single nucleotide polymorphisms (SNPs), determined with 3-enzyme restriction site-associated sequencing (3RAD) (Bayona-Vásquez *et al.* 2019, Glenn *et al.* 2019). Inbreeding estimated with genomic markers was shown to more strongly

predict identity by descent and decrease in fitness, compared to the pedigree (Hemmings *et al.* 2012b, Kardos *et al.* 2015, Huisman *et al.* 2016). First, because the genome of the aquatic warbler is not yet available, we constructed a reference genomic library according to the Reduced-Representation Single-Copy Orthologs (R2SCOs) method, following Driller *et al.* (2021), with modifications (see below). This method allows the construction of a catalogue of reliable loci excluding potential paralogs and loci with artefactual alleles. Three female samples with high DNA concentration (75.9, 53.7 and 76.6 ng/µl), each representing a different study location, were used. After normalising the samples to 20 ng/µl, we split each into five digestion reactions (200 ng each), totalling 1 µg digested DNA. The enzymes XbaI, EcoRi-HF and NheI were used for the digestion. The digestion ran at 37°C for two hours. Each digestion reaction was ligated with a unique iTru XbaI and EcoRI adapter pair (i.e. double-indexed). The five reactions of each sample were pooled and purified (PCRclean magnetic beads - GCbiotech) with 0.8x beads. We performed a PCR with P5 and P7 customised ligation check primers, to ensure that the digestion was successful. Each pooled sample was size-selected (350-580 bp) on a BluePippin machine (Sage Science). Each size selection product was then split into four reactions and in a single-cycle PCR we added an iTru5-8N index (with 8 random nucleotides to mark unique DNA template molecules and allow to remove PCR duplicates during the bioinformatic analysis). After purification (0.8x beads) an additional PCR step (eight cycles) completed the Illumina adapters with a unique iTru7 P7 primer per reaction. The four PCR replicates of each sample were then pooled, purified (0.8x beads) and quantified (Qubit – Thermo Fisher Scientific). Finally, the pools were sequenced with the Illumina MiSeq V3 at 600 cycles, yielding a total of 3.6 M reads per sample.

Next, we constructed population libraries, consisting of the remaining samples, following the protocol described above (Bayona-Vásquez *et al.* 2019). DNA concentration was measured with a Picogreen (Invitrogen) or Qubit (Thermo Fisher Scientific) device and normalised to 20 ng/ul. In total, we produced nine population libraries, which were processed in three batches (see Supplementary Online Material 1). The next steps followed the 'reference' protocol, with the exception that: 1) a size range of 350-500 bp was excised with Blue Pippin for Lib1-Lib6; 2) the size selection for Lib4, Lib5 and Lib6 was done after the indexing PCR and lacked the step of a single-cycle PCR adding a Itru5-8N primer; 3) for Lib4, Lib5 and Lib6 purification was carried out with AmPure beads; and 4) the number of cycles in the final indexing PCR was 12. Sequencing was done as follows: Cat1, Cat2, Cat3 and Lib3 – Illumina NextSeq MidOutput 300 cycles; Lib1 and Lib2, as well as Libs 4-6 – Illumina NovaSeq 6000 300 cycles, one lane of the SP flow cell; 15% of PhiX was used. The number of sequenced reads obtained from each library is presented in Table S1a.

Bioinformatic analysis

We first constructed a reference locus catalog using the R2SCOs method following Driller *et al.* (2021). Considering that there is no genome available for the aquatic warbler, the R2SCOs method allowed us to select a set of high-quality single-copy orthologous loci to be used as reference for the population analysis. We sequenced 2x300 bp reads for three females from the three locations to reconstruct the entire locus by merging overlapping reads. We followed the R2SCOs pipeline, which included de-replication of the pre-processed and size-selected (range 250-370 bp, for which we obtained comparable and high coverage) sequences, setting the minimum coverage per unique sequence to define a putative allele equal to three; and clustering and definition of putative loci using the intra-specific identity threshold of 90%. As a next step, the pipeline applies a set of filters to remove loci that are prone to generate spurious results due to issues of either biological or technical background. Aiming to avoid sex-biased genotypes that might interfere with the population analyses (Faux *et al.* 2020), we removed all the R2SCOs loci that mapped to the sex chromosomes of the Eurasian blackcap (*Sylvia atricapilla*) genome (GenBank accession number GCA_009819655.1), which was the closest related species with chromosomal-level genome available. The final reference contained 10,997 loci.

The raw data from the population libraries was mapped against the PhiX genome to filter any remaining read from the Illumina library control, which was added in the sequencing run to increase sequence diversity. Next, we performed adapter trimming using the Cutadapt software (Martin 2011). Then, reads were attributed to individuals based on the in-line barcodes using FLEXBAR (Dodt *et al.* 2012). PCR duplicates (only for Lib1, Lib2 & Lib3) were filtered out using the Python script Filter_PCR_duplicates.py (https://github.com/BeGenDiv/Arantes_et_al_2020). The four replicates were then concatenated. The forward and reverse reads were merged with overlapping regions of at least 30 bp and maximum length of 249 using the software PEAR (Zhang *et al.* 2014). All the merged reads (<249 bp) were considered short fragments that were out of the target range, and we continued analysing the unassembled read pairs, which were filtered for minimum quality (Q>30) and trimmed to 142 bp with a minimum length of 130 bp using Trimmomatic (Bolger *et al.* 2014). We checked the presence of the XbaI and EcoRI restriction sites in the paired-read ends using the script checkRestrictionSites.py (https://github.com/BeGenDiv/Arantes_et_al_2020) and filtering out any fragment resulted from star activity or NheI digestion. Finally, reads containing the internal restriction site of XbaI, EcoRI or NheI were removed using the Filter_Reads.py script (https://github.com/BeGenDiv/Arantes_et_al_2020). The filtered reads were mapped against the reference locus catalog constructed with the R2SCOs method. We performed mapping in Bowtie2 (Langmead *et al.* 2009) with default parameters and the flags '-no-mixed' and '-no-discordant'. In order to select a common range of high-coverage loci for all individuals belonging to different libraries, we checked the length distribution of the loci based on the .sam files, and selected the range 250-310 bp, which we then extracted from the .sam files with the Samtools and an 'awk' command.

We analysed the mapped reads with Stacks (Catchen *et al.* 2011, 2013), using the reference-based pipeline. Genotypes were called and filtered with *the ref_map.pl* programme, which utilises the *gstacks* and the *populations* modules. In *gstacks*, the *var_alpha* (alpha threshold for discovering SNPs) was set to 0.01, and all the samples were assumed to belong to one population, because of the extensive gene flow known in the aquatic warbler (Kubacka *et al.* 2023). Otherwise, default parameters were used. In *populations*, we used: the minimum percentage of individuals in a population required to process a locus for that population r= 0.8; the minimum number of populations a locus must be present in to be processed p= 1; and the minimum minor allele frequency required to process a nucleotide site at a locus min-maf= 0.005. We assumed r= 0.8 to avoid high levels of missing data and a min-maf of 0.005 following the recommendation that an allele should be present in at least three samples to be processed as a locus (Rochette & Catchen 2017). To obtain independent SNPs, we used the option of writing the first SNP in a locus. The remaining parameters were retained at their defaults. After calling genotypes, with Vcftools (Danecek *et al.* 2011), we generated mean depth per individual, to inspect coverage distribution. We removed three individuals with mean depth <10 and repeated the SNP-calling step without them. We ultimately obtained 6,267 loci, of which 4,179 variant sites (SNPs) were retained after the filtering with *populations*, with mean ±SE observed heterozygosity in variable positions of 0.141 ±0.002. In addition, we checked whether individuals with the lowest coverage (mean depth of at least 10 and <30 reads, N= 46) affect the loci-calling, by running *ref_map.pl* without them. The number of SNPs called without these individuals was 4,171 and the mean ±SE observed heterozygosity was 0.143 ±0.002; we therefore retained these individuals for further analysis. We then used Vcftools to inspect the SNPs and perform filtering (Table S1b). First, we generated mean depth per SNP with Vcftools and inspected its distribution. With the *minDP* option we removed genotypes with depth lower than 10 reads. Because these genotypes were turned to missing, with the *max-missing* option we filtered out loci with more than 20% missing data. Next, using the *max-mean-DP* option we filtered out sites (N= 6) of mean depth >115, to remove potential collapsed paralogs. We then identified SNPs that did not conform to Hardy-Weinberg (HW) proportions, by creating a file with HW equilibrium test p-values (Wigginton *et al.* 2005) using the *hardy* option. Next, we applied the false discovery rate (FDR) correction with the *p.adjust* command in the R environment (R Core Team 2023), and removed the SNPs with the FDR-adjusted p-values below 0.05. Finally, using the *--interchrom-geno-r2* option, we calculated loci-pairwise r^2 to inspect distribution of linkage disequilibrium. Mean ±standard deviation r^2 was 0.003±0.012. We excluded one randomly selected SNP from each pair for which r^2 was >0.3, to remove the tail of r^2 distribution (Fig. S1).

Determination of inbreeding and inbreeding load

We quantified the inbreeding rate with the inbreeding coefficient *F* calculated with a method of moments (Wang 2014) using the *–het* option in VCFtools (Danecek *et al.* 2011). To explore how well this metric corresponded to inbreeding, with the R package *inbreedR* (Stoffel *et al.* 2016), we calculated g_2, an estimate of identity disequilibrium (ID) which quantifies the covariance of heterozygosity at the studied loci standardised by their average heterozygosity; hence, it corresponds to inbreeding variance in the population (David *et al.* 2007). A correlation between a trait and heterozygosity will not arise when g_2=0 (Szulkin *et al.* 2010). We used 1,000 permutations over SNPs to evaluate whether g_2 is greater than zero and 100 bootstraps over individuals to determine its 95% confidence interval.

To quantify the strength of inbreeding depression, we used two metrics: the inbreeding load and percent change in a fitness trait due to inbreeding (Morton & Crow 1956, Keller & Waller 2002). Assuming that mutations at different loci have independent effects on fitness, the logarithm of a fitness-related trait is predicted to show a linear negative relationship with the inbreeding coefficient *F*. The inbreeding load *B* is quantified as the negative of the slope of the function describing this relationship. The effect of a mutation on fitness can be lethal (e.g. causing death of an individual) or have partial detrimental effects. To compare mutation effects on fitness-related traits between populations, the concept of lethal equivalents was coined. A lethal equivalent is referred to as the average number of alleles in a population which, when in the homozygous state would cause death of the homozygous individual. The inbreeding load *B* equals the average number of lethal equivalents per haploid gamete found in the studied population. We calculated *B* as the negative of the unstandardised, model-averaged estimate of the inbreeding effect on each of the analysed fitness-related traits (see below), and using models with the logarithm link function, which was shown to yield unbiased estimates of inbreeding load (Nietlisbach *et al.* 2019). For the purpose of *B* calculation, we used the Poisson distribution for the survival traits and the male reproductive success models, and the gaussian distribution for the remaining reproductive traits models (Nietlisbach *et al.* 2019). Percent change in fitness δ refers to the change in a fitness-related trait in inbred individuals compared to outbred individuals (Keller & Waller 2002). Because in our dataset we used a correlational coefficient of inbreeding, and were not able to assign individuals to inbreeding classes (e.g. outbred and born to siblings), we calculated δ for the most inbred individuals compared to the least inbred individuals in the considered dataset, as e.g. in the work of (Harrisson *et al.* 2019, Sin *et al.* 2021).

Quantification of fitness- and condition-related traits

We determined inbreeding depression on the following traits life-history and condition traits, which are likely to be determined by a large number of genes, and are thus expected to be affected by inbreeding (Chapman *et al.* 2009, Szulkin *et al.* 2010).:

(1) *Male long-term survival*. This trait was measured by the number of years during which a given individual was resighted or recaught in the study plots, over four years following the first observation year as a sexually mature individual (i.e. at least in its 2nd calendar year of life). We did not consider the female long-term survival due to the low number of female re-observations (8 recoveries out of 105 ringed females), which did not ensure a reliable regression analysis (Harrell 2015).

(2) *Male seasonal breeding success.* Further referred to as 'male breeding success', it was measured by calculating the number of offspring for each male by paternity assignment to 9-day-old chicks (i.e. those from which we obtained blood samples), over the breeding season in which the male was first sampled (i.e. either 2017 or 2018). In the aquatic warbler, nestling mortality takes place mostly within the first few days after hatching and the daily nest survival rate is high (Dyrcz & Zdunek 1993b, Kubacka *et al.* 2014). Therefore, the number of 9-day-old offspring is a suitable proxy of the male breeding success. To determine chick paternity, we first selected a set of informative SNPs to maximise the statistical power of parentage assignment, following recommendations in (Andrews *et al.* 2018, Thrasher *et al.* 2018). With Vcftools (Danecek *et al.* 2011), we filtered out SNPs with minor allele frequency (MAF) below 0.3 and missing data per SNP exceeding 0.1. We selected the MAF threshold of 0.3, because rare SNP variants do not provide useful information in parentage assignment (Huisman 2017). The genotypes file consisted of 333 SNPs (Table S1b). For parentage assignment (as opposed to methods relying on exclusion) performed with SNPs typically 100-200 markers suffice (Huisman 2017, Flanagan & Jones 2019). For one individual, which was RAD-sequenced twice, we removed the genotype with fewer loci typed. We retained the genotypes of four individuals that were RAD-sequenced both as chicks and adults, and duplicated the genotype of one individual that was observed both as a chick and an adult but RAD-sequenced once, to allow these individuals being both parents and offspring. The resulting genotypes dataset consisted of 320 offspring (316 with known mother) and 175 candidate fathers, with one mother typed in 88 SNPs and all the other individuals typed in at least 100 SNPs. Paternity was then assigned with Cervus (Kalinowski *et al.* 2007), using the three modules: allele frequency analysis, parentage analysis simulation and paternity analysis given known mother. The allele frequency analysis showed the mean proportion of SNPs typed of 0.954. In the parentage analysis simulation, we assumed: the allele frequencies generated in the previous step; 100,000 offspring (as

recommended to obtain reliable critical values of Delta at high levels of confidence); 440 as the average number of candidate fathers per offspring (based on the number of males assessed within the study plots and 150 m around them, and summed over all the three study locations); 0.4 as the proportion of candidate fathers sampled; 0.954 and 0.01 as the proportion of loci typed and mistyped, respectively; 0.01 as the error rate in likelihood calculations; 88 as the minimum number of typed loci; Delta as the statistic to determine confidence; and 99% and 95% as the strict and relaxed confidence level, respectively. In the paternity analysis, we used the allele frequency and simulation results generated in the previous steps. The offspring file contained information on candidate fathers.

We obtained a low father-to-offspring assignment rate (see Results), which could have been caused by the unassigned males being far from the nearest genotyped nests. Therefore, we used QGIS 3.10.7 to determine 1) distances between fathers and nests with their young, taking averaged coordinates of captures and subsequent resightings of the males; and 2) distances of the males unassigned paternity to the nearest genotyped nest. In addition, based on all the captures and resights of the males in our study area, we determined the number of encounters of a male in a plot throughout each breeding season. Individuals with a low number of encounters were first captured during the second breeding attempt or were rarely seen in the study plots. We used the number of encounters to decrease unexplained variation in the male breeding success (see below).

(3) *Clutch size*. Referred to as the observed or deduced number of eggs in nests found at the egg stage or with nestlings aged below three days. During the first two days after hatching chances are high that the weakest nestlings are still alive, while after this timepoint there is a risk that they have died and were removed by the female, thus biasing the inference on clutch size.

(4) *Hatching failure*. Determined with the number of eggs that hatched and the number of eggs that did not hatch, with the egg being treated as the subject.

(5) *Nestling mortality*. Quantified with the number of nestlings that survived until fledging (see point 6 below) and the number of nestlings that died before fledging, out of all the nestlings that hatched and with the individual nestling being the subject. Nestling mortality was determined only for the nests found at the stage of eggs or before day 3 post-hatch, to minimise the bias due to missed early chick mortality (see point 3 above).

(6) *Fledged brood size in successful nests*. Further referred to as 'fledged brood size'. Determined as the number of nestlings seen on the last nest check when brood was still in the nest, as long as on the following check the nest did not bear any traces of predation (e.g. dead chicks or their parts, torned nest, feathers around) and the nest was recorded empty not earlier than on day 12 post-hatch (the average fledging time is 15 days post-hatch, Kubacka pers. inf., (Dyrcz 1993)).

(7) *Chick tarsus length*. Obtained by measuring the distance from the notch on the metatarsus to the top of the bone above the folded toes, with a calliper to the nearest 0.1 mm. Tarsus measurement was taken on days 2, 5 and 9 post-hatch. In birds, tarsus length is one of the proxies for structural body size (Rising & Somers 1989, Senar & Pascual 1997).

(8) *Chick body reserves.* Determined with the scaled-mass index (SMI) using a custom script (https://gist.github.com/chenpanliao/8ef652404d024c2c4191b8f159400a37) in the R environment v. 4.3.2 (R Core Team 2023). SMI is a proxy for relative energy reserves, and is quantified with the body mass and a measure of body length (Peig & Green 2009), for which we used the tarsus length (see point 7). In passerines, SMI corresponds to the amount of subcutaneous fat (Peig & Green 2009, Nip *et al.* 2018).

Statistical analysis

We ran the analysis in the R environment v. 4.3.2 (R Core Team 2023) and applied the information-theoretic approach, in which an a priori set of biologically plausible candidate models is built and each model in the set obtains a relative rank indicating how well it explains the data (Burnham & Anderson 2002). To rank models within a candidate set, we used the Akaike information criterion corrected for small sample size (AICc). In addition, we generated the following quantitative measures of relative support for each model: model likelihood (relative likelihood of the model in the candidate set, given the data), Akaike weight (ωAICc; probability that the given model is the best approximating model in the candidate set), evidence ratio (showing the probability of the best model relative to other models in the set) and cumulative AICc (sum of AICc weights of a given model and all the higher-ranking models) (Symonds & Moussalli 2011).

We constructed the candidate model sets as shown in Tables S2, S4, S7 & S9. Each candidate set included a null model (i.e. one assuming that the response variable is constant). For selected candidate sets, we restricted the number of variables in a model to allow approximately 10 data points per each non-intercept estimate and reduce the risk of over-parametrisation; for models using the binomial distribution, we ensured that there are approximately 10 data points of the less probable event per estimate (Harrell 2015). To account for model uncertainty, for each variable we calculated the average estimate and confidence intervals weighted by the ωAICc of each model in a set that contained the variable (i.e. natural model-averaging), as we expected small effects (Grueber *et al.* 2011, Symonds & Moussalli 2011). Model selection and averaging were carried out with the package *AICmodavg* (Mazerolle 2019). All the numerical explanatory variables were standardised to a mean of zero and an SD of one using the *scale* function from the *base* package.

To estimate inbreeding depression, we evaluated the relationship between the individual inbreeding coefficient and the fitness- and condition-related traits (response). In order to determine whether inbreeding depression is conditioned by phenotypic and environmental variables, we also evaluated support for their interaction with inbreeding rates. The relationships assessed and the candidate model sets were as follows:

(1) *Male inbreeding and long-term survival rate*. This candidate set was constructed using generalised linear models with Poisson error structure and log-link, fitted with the *glm* function from the *stats* package. We included tarsus and wing length, as well as their quadratic terms as covariates (Table S2a).

(2) *Male inbreeding and seasonal breeding success*. As observed previously (Dyrcz *et al.* 2005), the distribution of the male breeding success in the aquatic warbler is right-skewed and has a large number of zeros. This was also the case with the male breeding success in our dataset, which required choosing a model structure that accounts for this distribution. To this end, we first explored overdispersion and zero-inflation in the male breeding success. We determined the index of dispersion (i.e. variance to mean ratio, VMR) and the index of zero-inflation (ZI), both with respect to the Poisson distribution (Puig & Valero 2006), and their bootstrapped 95% confidence intervals (Cis) using the *boot* and *boot.ci* functions from the *boot* package (Davison & Hinkley 1997, Canty & Ripley 2021) and the 'basic' option. The VMR was 4.8 (95% CI 3.5 to 6.4), indicating overdispersion in the male breeding success, and the ZI was 0.7 (95% CI 0.6 to 0.8), indicating that it is zero-inflated with respect to the Poisson distribution. We then calculated the index of zero-inflation with respect to the negative binomial distribution (Blasco-Moreno *et al.* 2019), which was 0.2 (95% CI –0.04 to 0.50), indicating no zero-inflation with respect to the negative-binomial distribution. Next, to select the most appropriate count model (Blasco-Moreno *et al.* 2019, Campbell 2021), we compared a Poisson (P), a negative-binomial (NB), as well as zero-inflated models with the Poisson (ZIP) and the negative-binomial (ZINB) distribution in the count model. In each model, the male breeding success was the response variable and the male inbreeding coefficient, tarsus length and wing length, their quadratic terms and interactions with male inbreeding, study area, ringing year and the number of encounters in a study area were explanatory variables. We fitted the P model using the *glm* function from the *stats* package, the NB model with the *glm.nb* function from the *MASS* package (Venables & Ripley 2002), and the ZIP and ZINB models using the *zeroinfl* function from the *countreg* package (Zeileis *et al.* 2008, Zeileis & Kleiber 2022). The zero-inflated model is a mixture model that assumes presence of excess zeros in the data and allows the zeros to be of two kinds. It comprises a binomial model with log-link (modelling the point mass zeros) and a count model with log-link (modelling a response that can take values of zero or greater) (Zeileis *et al.* 2008, Green

2021). In our analysis, the binomial model estimated the probability that a male did not produce any 9-day-old young in our study plots, for example because it had a large home range or arrived in the study area only for the second breeding attempt. In the binomial model of the zero-inflated models we included only the number of encounters as the explanatory variable. The count model estimated the male breeding success, allowing for producing no young, e.g. due to low fertility, sperm competition, post-copulatory female choice or inefficient female guarding. We ranked the models by three information criteria, AICc, AIC and BIC (Campbell 2021). The NB model obtained the highest support as indicated by the lowest values of all the information criteria (AICc= 377.5, AIC= 374.8, BIC= 413.8.0), compared to the ZINB (AICc= 379.6, AIC= 376.4, BIC= 418.4), ZIP (AICc=394.1, AIC= 391.3, BIC=430.3) and P model (AICc= 522.9, AIC= 520.6.0, BIC= 556.6). Therefore, we proceeded with the negative-binomial models to construct a candidate set. We included tarsus and wing length as well as their quadratic terms and interactions with the inbreeding coefficient, and number of encounters as covariates (Table S2b).

(3) *Female inbreeding and clutch size*. This candidate set was constructed using linear models (function *lm*). As covariates, we included the mother tarsus and wing length as well as their quadratic terms, laying date (present in each model except the null model, as it strongly predicts the clutch size), sum of rainfall averaged for 15 days prior to start of incubation, minimum daily ground temperature and maximum daily temperature averaged for 15 days prior to start of incubation, and the interactions of the covariates with the mother inbreeding coefficient. The study area and nesting year were added to the models as fixed categorical factors. We restricted the number of non-intercept estimates in a model to six (Table S4a).

(4) *Female inbreeding and the egg hatch failure*. This candidate set was built using general linearised models (function *glm*) and the binomial distribution with logit link. We coded hatched egg as 0 and unhatched egg as 1. As covariates, we included the laying date, sum of rainfall during incubation, minimum daily ground temperature and maximum daily temperature averaged over the incubation stage and clutch size; study area and nesting year were included as above. Due to the low number of unhatched eggs (N=23), we limited the number of non-intercept estimates in a model to two and did not consider interactions (Table S4b).

(5) *Female inbreeding and nestling mortality*. This candidate set was constructed with generalised linear models (function *glm*) and the binomial distribution with logit link. A nestling that survived until fledging was coded as 0, and one that did not survive was coded as 1. As covariates, we included the wing and tarsus length of the mother, laying date, sum of rainfall from the hatch day until the last day when chicks were seen in the nest, minimum daily ground temperature and maximum daily temperature averaged over the nestling stage

as above, and hatched brood size; study area and nesting year were included as above. Due to the low number of nestling deaths (N=22), we limited the number of non-intercept estimates in a model to two and did not consider interactions (Table S4c).

(6) *Female inbreeding and fledged brood size in successful nests*. This candidate set was built using linear models (function *lm*). We analysed only successful nests (i.e. those broods that failed due to predation on nest or female), as nests are predated for reasons that are mostly independent of the female. As covariates, we included mother wing and tarsus length as well as their quadratic terms, laying date, sum of rainfall from the hatch day until the last day when chicks were seen in the nest, minimum daily ground temperature and maximum daily temperature averaged over the nestling stage as above, and interactions of the covariates with the mother inbreeding coefficient; area and year were included as above. The number of non-intercept estimates in a model was limited to seven (Table S4d).

(7) *Nestling and mother inbreeding, and nestling tarsus length on days 2, 5 and 9 post-hatch*. We built this candidate set using general linear mixed models fitted with the *lmer* function from the *lme4* package (Bates *et al.* 2015), and without REML. Mother ID, chick ID and father ID were entered as random intercepts. We included covariates and factors as follows: chick sex, brood size, laying date, sum of rainfall in the 14 days preceding the day of measurement, minimum daily ground temperature and maximum daily temperature averaged over four days preceding the day of measurement, and amount of preferred prey around the nest (Table S7a). The amount of preferred prey was the total number of insects from the taxonomic groups known to be frequent in food brought by female aquatic warblers to nestlings: *Odonata*, *Aranea*, *Lepidoptera* and *Orthoptera* (Schulze-Hagen *et al.* 1989, Kubacka in prep.).

(8) *Father inbreeding and nestling tarsus length on days 2, 5 and 9 post-hatch*. We constructed this candidate set using general linear mixed models fitted as detailed under (7) above (Table S7b). We evaluated the effect of father inbreeding in a separate candidate set due to incomplete father-to-offspring assignment (see Results), which created missing data for father inbreeding in the chick dataset.

(9) *Nestling and mother inbreeding, and nestling SMI on days 2, 5 and 9 post-hatch.* This candidate set was constructed as detailed under (7) (Table S9a).

(10) *Father inbreeding and nestling SMI on days 2, 5 and 9 post-hatch.* This candidate set was built as detailed under (8) (Table S9b).

We visualised results with the package *ggplot2* (Wickham 2016) using model-averaged estimates (see above) and predictions averaged over all the levels of the categorical factors with the packages *AICmodavg* (Mazerolle 2023) and *MuMIn* (Bartoń 2019), and custom code (https://philippmasur.de/2018/11/26/visualizing-interaction-effects/).

Results

RAD-seq, inbreeding statistics and parentage assignment statistics

The number of reads obtained per library are summarised in Table S1a. The final resulting number of SNPs after filtering was 2,948 (Table S1b). The mean ±SD read depth per locus and individual was 77.5 ±17.0 and 77.5 ±38.8, respectively, and the median ±SD frequency of missing genotypes per individual was 0.014, range 0.001 to 0.725 (Fig. S2).

In parentage assignment, we obtained the range and median number of mismatches of 0-3 and 0 for social mothers; and 0-5 and 1 for the trios in which fathers were assigned with 99% confidence, excluding the male for which pair confidence did not reach 99% confidence (see below). The number of trio loci mismatching for trios containing the second most likely father had a median of 39 and range 17-49. We obtained an offspring assignment rate of 70% (225/320 offspring), and 33% (58/175) males were assigned paternity with both the pair (i.e. father-offspring) and the trio (i.e. father-mother-offspring) confidence of 99%, except for one case in which the mother was not sampled and trio confidence could not be determined. We excluded one assignment, for which the trio confidence was 99%, but the pair confidence was below 95%. This assignment was made between a male and a nest that were over 3 km apart.

We obtained inbreeding coefficients *F* of mean ±sd 0.005 ±0.043, median 0.001 and range –0.077 to 0.138 for adult females; mean ±sd 0.029 ±0.048, median 0.031, range –0.10 to 0.17 for adult males and mean ±sd 0.004 ±0.056, median 0.005 and range –0.431 to 0.175 for offspring (Fig. S3). Two nestlings obtained very low inbreeding coefficients and we removed them from the tarsus and SMI analysis as outliers. The *g2* was estimated at 0.0009 (95% confidence interval 0.0005 to 0.001) and was greater than zero (*P*= 0.001) (Fig. S4), which indicated an inbreeding genome-wide effect, i.e. that different loci within an individual covary in heterozygosity.

Fitness-related trait statistics

Of the 178 males ringed between 2017-2019, the mean ±SD return rate over four years was 0.6 ±1.0 years (median 0, range 0-4). The breeding success of the males had a mean of 1.0, median of 0 and range 0 to 12. Females laid on average ±SD 4.7 ±0.7 eggs, with the mean egg hatch failure of 0.06, mean nestling mortality before fledging of 0.11, and mean ±SD fledged brood size in successful nests of 4.1 ±1.1.

Relationship between adult inbreeding coefficient and fitness components

In adult males, the return rate was predicted neither by their inbreeding coefficient, nor by its interaction with tarsus length and wing length (Fig. 1, Table S3a). The model assuming a constant return rate obtained the highest support of all the candidate models (ωAICc=0.74) (Table S2a). The return rate had an inverse quadratic relationship with tarsus length, indicating that it is the highest for males with average tarsus length (Fig. 1, Table S3a).

While the male inbreeding coefficient was not a good predictor of the seasonal breeding success for the average value of the phenotypic covariates (Fig. 1, Table S3b), the model considering that its statistical effect interacts with male tarsus length obtained the highest support (ωAICc=0.45). This model was also 2.1 times more probable than the null model (ωAICc=0.22) and 6.6 more probable than the model without the tarsus by inbreeding interaction term (ωAICc=0.07) (Table S2b). In males with small tarsi, the estimate of the inbreeding effect was weakly negative, and in males with exceptionally large tarsi it was positive, however, the latter result was based on very few observations and estimated with high uncertainty (Fig. 2). In other words, in males with small tarsi, a higher inbreeding coefficient corresponded to a lower breeding success, while in majority of males with large tarsi a relationship between their inbreeding rate and breeding success was not supported. The number of encounters of a male within the study plot positively correlated with his breeding success (Fig. 1, Table S3b).

For the average value of the covariates, the effect of female inbreeding rate on the clutch size was estimated at close to zero and had a broad confidence interval (Fig. 3, Table S5a). However, the model considering that the inbreeding coefficient interacts with tarsus length obtained top support and was about three times more probable than the model without this interaction term (Table S4a). In females with small tarsi, the statistical effect of inbreeding on the clutch size was negative, while in those with the largest tarsi it appeared positive; however, again, the latter result was based on very few observations and thus uncertain (Fig. 4). For the females with tarsi shorter than average, with one standard deviation increase in the inbreeding coefficient the clutch size decreased by 0 to 0.75 egg (Fig. 4). In addition, the inbreeding coefficient effect interacted with the average maximum daily temperature during two weeks before incubation (Fig. 3, Table S5a). As the maximum temperature increased, the statistical effect of the female inbreeding rate on clutch size became more negative, however, its confidence intervals spanned zero along the temperature ranges (Fig. 4). The clutch size decreased with the laying date, increased with the female tarsus and wing length, and showed an inverse quadratic relationship with these traits ((Fig. 3, Table S5a).

Female inbreeding rate showed no clear relationship with hatch failures, nestling mortality and fledged brood size in successful nests, and neither was its statistical effect modified by wing length and the environmental covariates – incubation start date, minimum and maximum

temperatures and rainfall (Tables S5b-d, Fig. 3). The hatch rate model selection indicated the null model as the highest ranking one (ωAICc=0.22) (Table S4b). The nestling survival rate model selection showed that the minimum and maximum temperatures are important predictors of nestling mortality, indicating higher survival in higher temperatures (Table S4c, Table S5c, Fig. 3). Nestling mortality increased with the hatched brood size, indicating a negative effect of sibling competition (Table S5c, Fig. 3). The fledged brood size in successful nests was positively predicted by mother wing length and decreased as the breeding season progressed (Table S5d, Fig. 3). The model assuming change of the fledged brood size by mother inbreeding and incubation start date scored first (ωAICc=0.25), and the AICc weight of models containing the latter totalled 0.45, showing that incubation start date is an important predictor of the fledged brood size (Table S4d).

Relationship between nestling and parental inbreeding coefficient, and nestling condition

In the candidate set examining effects of chick and mother inbreeding, the model assuming that the mother inbreeding rate interacts with the average maximum daily temperature over the previous four days scored first with very strong support (ωAICc=0.99) (Table S7a). This interaction indicated that as the maximum temperature increased, the effect of the mother inbreeding rate on chick tarsus became more negative (Fig. 7). There was also a similar but weaker effect of the average minimum ground temperature by mother inbreeding rate, which could have the same interpretation, as the two temperatures were correlated, and the minimum temperature weakly interacted with the chick inbreeding rate with a similar pattern (Fig. 5, Table S6). The mother inbreeding rate interacted with the day of tarsus measurement, which indicated that on day 9 it has a weak negative effect on chick tarsus relative to day 2 (Fig. 5, Table S6, Fig. 6). While the chick and mother inbreeding rates had negative estimates, their confidence intervals spanned zero and therefore evidence for their relationship with nestling tarsus was very weak (Fig. 5, Table S6).

In the candidate set evaluating effects of the father inbreeding rate on chick tarsus, the model considering that the father inbreeding coefficient interacts with the maximum temperature obtained top and strong support (ωAICc=0.82), being over 17 times more probable than the next high-ranking model (Table S7b). Similarly to the pattern that we found in females and chicks, the father inbreeding rate had a more negative effect on chick tarsus as the maximum temperature increased (Fig. 7). It is worth noting that the strength of this effect was higher compared to that in mothers and chicks (Fig. 5, Table S6). In addition, the statistical father inbreeding effects on chick tarsus became increasingly negative as chicks grew older, being lower than zero on days 5 and 9, and this effect was more than twice stronger compared to the mother inbreeding coefficient by day effect (Table S6, Fig. 5, Fig. 6). The father inbreeding coefficient statistical effect also interacted with the laying date, becoming more negative for broods initiated later in the season (Table S6, Fig. 5, Fig.

7). While the main effect of father inbreeding rate on offspring tarsus was more negative compared to that of the mothers and chicks, its confidence interval also overlapped zero (Table S6, Fig. 5).

A weak positive interaction effects between the chick inbreeding coefficient and the minimum ground temperature as well as rainfall were supported, indicating that chick inbreeding coefficient has more negative effects on SMI in lower than in higher minimum ground temperatures and rainfall levels (Fig. 5, Fig. 7, Table S8). In addition, a weak negative interaction effect between the mother inbreeding rate and maximum temperature was present, showing that the mother inbreeding effect is more negative in higher than in lower maximum temperatures (Fig. 5, Fig. 7, Table S8). We did not find support for an association between nestling inbreeding coefficient and SMI. The effect of nestling inbreeding was also not found to differ between days 2, 5 and 9 post-hatch, as indicated by the inbreeding effect by day interaction estimates with confidence intervals overlapping zero (Table S8, Fig. 5). Similarly, we obtained low evidence for a relationship between the mother or father inbreeding rate and nestling SMI and for the interactions between chick, mother and father inbreeding and the remaining environmental variables (Table S8, Fig. 5).

Inbreeding load

The males with small tarsi incurred strong inbreeding load and those with large tarsi were not found to carry inbreeding load and even appeared to benefit from being inbred – although the confidence intervals of their *B* estimate overlapped zero (Table 1). The decrease in this trait in the most inbred small males was high relative to the least inbred ones, with an estimated 75.7% (Table 1). For the average tarsus and wing, the inbreeding load on male return rates was low and its confidence intervals overlapped zero; likewise, change in fitness for the most inbred adult males in our dataset, relative to the least inbred, was negligible (Table 1). Similarly, for the average tarsus and wing the inbreeding load on the male seasonal breeding success was low and its estimate's confidence intervals also overlapped zero.

The change in clutch sizes for the most inbred small females, relative to the least inbred small females, was 9.5% and involved 0.7 lethal equivalents (Table 1). The relationship between adult female inbreeding and female clutch sizes, hatching failure, nestling mortality and fledged brood size in successful nests was associated with low inbreeding load estimates, the confidence intervals of which overlapped zero. Consequently, the overall decrease in fitness between laying a clutch and brood fledging was low, for mean values of all the phenotypic traits studied, amounting to 0.5 haploid lethal equivalents (Table 1).

The change in nestling tarsus length and SMI on days 2, 5 and 9 post-hatch in function of the chick and parental inbreeding was low. We found the strongest change for the chick tarsus, which

decreased due to the father inbreeding rate by 7.3-7.8% on days 5 and 9 in nestlings of the most inbred fathers, compared to the nestlings of the most outbred fathers (Table 1).

Discussion

Our study shows that in adult aquatic warblers, effects of female and male inbreeding, as determined with SNP markers and a method of moments inbreeding coefficient, on the clutch size and breeding success, respectively, are conditional on the structural body size, as measured with tarsus length. We also demonstrate that the effect of father inbreeding coefficient, and to a lesser extent so – that of mother inbreeding on chick structural body size growth is negatively conditioned by nestling age. Finally, we provide partial evidence for interaction of inbreeding rates with environmental conditions – maximum daily temperature, laying date and rainfall.

General effects of inbreeding

For the mean value of the studied phenotypic and environmental covariates, inbreeding depression on the long-term return rates and seasonal breeding success of adult males was not supported by our data. Male aquatic warblers show high post-breeding annual return rates of approximately 30% (Dyrcz & Zdunek 1993a, Bellebaum 2018), which is comparable to the annual survival of other migratory passerine birds in the central European latitude (Scholer *et al.* 2020). Hence, the four-year return rate is a proxy for their survival rate over the lifespan of most individuals. Our results suggest, therefore, that the inbreeding rate in adult males is not associated with their lifespan. We were not able to evaluate whether individual inbreeding is associated with the return rate of adult females. Female aquatic warblers are more difficult to detect, compared to males, and could be the more dispersing sex (Bellebaum 2018). Inbreeding depression on their adult survival rates awaits studies using, for example, lightweight tracking devices.

Inbreeding depression on adult survival has not been studied often. For example, in the song sparrow (*Melospiza melodia*), the inbreeding load on annual survival rates of adults was estimated at *B*= 1.7 (Keller 1998), and in helmeted honeyeaters (*Lichenostomus melanops cassidix*), the lifespan decreased by 49% in the most inbred compared to the least inbred females, but remained comparable in males (Harrisson *et al.* 2019). In the house sparrow (*Passer domesticus*), annual survival was negatively related to genomic inbreeding (Niskanen *et al.* 2020). The *B*= -0.2 that we found for adult male annual survival does not indicate inbreeding load on this trait in the aquatic warbler.

We also did not find support for inbreeding depression to act on another male fitness component, the seasonal breeding success. We studied the male seasonal breeding success during one breeding season for each male. While several individuals can breed only once, some will breed over two and even three or more breeding seasons. It was shown that weak negative inbreeding effects on short-term fitness traits cumulate into strong inbreeding load across consecutive life stages (Szulkin *et al.* 2007, Grueber *et al.* 2010, Harrisson *et al.* 2019). We detected a weakly negative effect of adult male inbreeding rate on male breeding success, which could grow to a strongly negative association over an individual's lifetime. Inbreeding depression on the male lifetime reproductive success in the aquatic warbler is therefore worth studying in the future. Other studies reported variable evidence for inbreeding depression on the male seasonal breeding success. In the helmeted honeyeater, the most inbred males produced 42% fewer fledglings per clutch and this relationship was weaker in females (Harrisson *et al.* 2019). In the Leach's storm-petrel (*Oceanodroma leucorhoa*) support was weak for effects of parental inbreeding rates on the breeding success (Sin *et al.* 2021). In the house sparrow, individual genomic inbreeding had a strong negative effect on the annual reproductive success and incurred a high cost of *B*= 6.4 (Niskanen *et al.* 2020).

Similarly to males, for the mean value of the studied phenotypic and environmental covariates, we found no support for the relationship between a female's inbreeding rate and her short-term fitness components: clutch size, offspring survival from egg to hatching, and from hatching to fledging, and fledged brood size (excluding mortality due to nest predation). Our estimates of low maternal inbreeding load on the studied reproductive traits do not support inbreeding depression on offspring production until fledging in the aquatic warbler. However, it is the earliest survival stages, especially at the egg stage, that could respond more negatively to inbreeding (Noordwijk & Scharloo 1981, Hemmings *et al.* 2012b), and inbreeding of the individual, as opposed to the inbreeding of a parent, could affect the survival fitness components more strongly. We could not acquire data on the inbreeding of unhatched embryos and young chicks before their death (which takes place mostly before day 9, when they were blood-sampled). In addition, evaluating offspring inbreeding through determining relatedness within the pair is difficult in the aquatic warbler, as this species does not form pair bonds. For this reason, we could not evaluate the relationship between the inbreeding and early survival of offspring. In future studies of inbreeding in the aquatic warbler it will be crucial to determine egg fertilisation and tissue-sample unhatched embryos and chicks immediately after hatching, to pinpoint the inbreeding depression taking place at these early developmental stages. In addition, inbreeding effects of the mother on fledged brood size could occur only in less favourable environmental conditions, for example due to lower food availability (Kruuk *et al.* 2001, Keller *et al.* 2002, Wilson *et al.* 2006). It will be important to evaluate inbreeding depression on the female lifetime reproductive success, which could be stronger (Harrisson *et al.* 2019).

Previous studies on birds found the first-kin parental inbreeding (e.g. due to parents being siblings) to be little related to the clutch size or total egg production (Keller 1998, Szulkin *et al.* 2007, Harrisson *et al.* 2019). In contrast, stronger evidence was found for maternal, or parental in general, inbreeding reducing survival to fledging and production of young (see also the examples above). In the takahe (*Porphyrio hochstetteri*), the parental inbreeding statistical effect on the hatching rates and fledging success was not found to differ from zero (Grueber *et al.* 2010). The inbreeding load due to first-kin parental inbreeding on hatch rates was estimated at B= –0.7, and that on the fledging rate was determined at B= 3.3 (Grueber *et al.* 2010). However, other authors found a negative association of maternal inbreeding with brood fledging success in this species, with inbred mothers (pedigree coefficient of inbreeding f>0) producing approximately 30% fewer fledglings compared to outbred mothers (f=0) (Jamieson *et al.* 2003). In the song sparrow, first-kin maternal inbreeding led to a 36% reduction in the clutch hatching success and was negatively related to the number of independent young (Keller 1998). In the helmeted honeyeater, the most inbred females suffered a 20% decrease of the clutch hatch rates and produced 26% fewer fledglings per clutch, compared to the least inbred ones (Harrisson *et al.* 2019).

We conclude that in the aquatic warbler the depression on reproductive rates and offspring survival rates related to mother inbreeding, and the depression on the seasonal breeding success and long-term survival associated with adult male inbreeding are low for average values of the phenotypic (wing length and tarsus length) and environmental (temperature, rainfall, brood size and laying date) covariates. Accordingly, the inbreeding load on these fitness components is low for the mean covariate values.

Conditional inbreeding depression in adults

We demonstrated that inbreeding depression on fecundity-related traits is conditional on the structural body size of males and females, as measured with tarsus length. In birds, tarsus length is a proxy for structural body size (Rising & Somers 1989, Senar & Pascual 1997). Therefore, our results imply that inbreeding costs on the seasonal breeding success increase in small-bodied males, and those on the clutch size increase in small-bodied females, relative to large-bodied individuals. Tarsus length in birds is heritable (Smith & Dhondt 1980, Dhondt 1982, Noordwijk *et al.* 1988, Potti & Merino 1994), but also affected by the environment at rearing, in particular egg size, food abundance, brood size, ectoparasite load, laying date or weather (Alatalo & Lundberg 1986, Noordwijk *et al.* 1988, Potti & Merino 1994, Merilä & Fry 1998, Kruuk *et al.* 2001, Liker *et al.* 2008, Andrew *et al.* 2017). Early developmental conditions also predict the adult body size in birds (De Kogel 1997, Searcy *et al.* 2004, Cleasby *et al.* 2011). Hence, the inbreeding depression on fecundity-related traits that is stronger in smaller-bodied individuals might suggest a negative carry-over effect of juvenile growth in an unfavourable environment, or of being born to small-bodied parents. When

environmental conditions at rearing are poor, offspring will be on average smaller, become on average smaller sexually mature adults, and could incur costs of inbreeding on fecundity in adult life. The proximate mechanism underlying the conditionality of inbreeding depression on these reproductive rates remains to be studied. Tarsus length is positively associated with the clutch size in females of some passerine birds (Sedinger *et al.* 1995, Garamszegi *et al.* 2004), including in the aquatic warbler (this study). In male zebra finches (*Taeniopygia guttata*) tarsus length is positively correlated with sperm quality and functionality traits (Forstmeier *et al.* 2017), and in male cliff swallows (*Petrochelidon pyrrhonota*) a body size index is positively related to the testis size (Brown & Brown 2003), which translates into sperm production (Parker & Pizzari 2010, Hayward & Gillooly 2011). Therefore, one hypothesis explaining the interaction between tarsus length and breeding success in male aquatic warblers could state that it is more difficult for small inbred individuals to compensate for their lower fecundity, than it is for small outbred ones. Alternatively, or additionally, inbreeding in small-bodied males could more negatively affect their breeding success through compromised female guarding, e.g. fewer copulations and less efficient deterrence of rivals. The inbreeding depression that we detected on the breeding success in the small-bodied males appears strong. For example, the *B* of 11 and ~76% decrease in the male annual reproductive success are comparable to the strong inbreeding depression on this trait found in the house sparrow (Niskanen *et al.* 2020). In small-bodied females, the inbreeding load on clutch sizes of about one lethal haploid equivalent and the decrease in the clutch size produced (~10%) were low to moderate and did not translate to decreased fledgling production, as shown by the unsupported interaction between the female tarsus and the female inbreeding coefficient on the fledged brood size. It appears that our finding of weak inbreeding depression in small females on their clutch sizes stands in contrast with results of previous studies (Keller 1998, Szulkin *et al.* 2007, Harrisson *et al.* 2019).

In sum, the tarsus by inbreeding interaction effects on female clutch sizes and the seasonal breeding success of males show that in the aquatic warbler (1) inbreeding depression on the clutch size and male seasonal breeding success depend on the body size; (2) inbreeding depression is stronger in small-bodied individuals relative to large-bodied ones with regard to these fitness components; (3) for the clutch size it is weak but clear in small-bodied females, but is not detected for fledged brood size in females of either body size; (4) for the breeding success, it is clear and strong in small-bodied males; and (5) external conditions at rearing could enhance inbreeding depression on these reproductive traits, which is a hypothesis to be tested in the future.

Conditional inbreeding depression on nestling growth

Chicks of more inbred parents, especially fathers, grew smaller until day 9 post-hatch compared to offspring of less inbred parents. These effects were weak to moderate (~2% for mother inbreeding

on day 9, and ~7-8% on father inbreeding on days 5 and 9) but clearly supported. It is worth noting that the association between nestling or parental inbreeding rate and nestling tarsus was unsupported for the youngest age when these traits were measured (day 2 post-hatch), as indicated by the confidence intervals of the day 2 by inbreeding interactions spanning zero (Fig. 5). This implies that it is not the initial offspring body size on which inbreeding costs are incurred, and that effects of parental inbreeding operate after hatching and become stronger with nestling age. Interestingly, the father inbreeding coefficient was more negatively correlated with offspring tarsus compared to the mother inbreeding rate, with the statistical effects being stronger both on day 5 and 9. The tarsus length of chicks had a similar association with their inbreeding rate as with the mother inbreeding rate, however, the statistical effect of the former obtained weaker support. Overall, this indicates slower growth in offspring of more inbred fathers and, to a lesser extent, of more inbred mothers, but not of more inbred offspring. As fathers do not tend nests in the aquatic warbler, effects of the father's inbreeding rate on chick tarsus can only be explained by the father's genetic make-up, and not by female food provisioning. In contrast, females are predicted to affect the growth of their offspring not only genetically, but also through maternal effects and prey acquisition performance, which could partly explain the weaker mother inbreeding effects on nestling tarsus.

Interestingly, we obtained support for interaction of the inbreeding coefficients with weather variables. Higher temperatures in the preceding days enhanced negative effects of nestling, mother and father inbreeding on nestling tarsus, with the strength of the interaction being the lowest in chicks, moderate in mothers and the strongest in fathers. Higher temperatures also made mother inbreeding effects on nestling SMI stronger, and chick inbreeding effects on SMI were more negative in lower temperatures and rainfall. An explanation linking the results with regard to chicks and mothers could be that elevated temperatures and/or low rainfall correlate with lower abundance of prey, which requires that females invest more energy into collecting food for young. In other words, it might be more difficult for females to compensate for negative effects of inbreeding in elevated temperatures and dry weather. With regard to fathers, we note that while both temperature and rainfall correlate with the laying date, the latter interacted with the male (with similar strength and the same direction of the effect), but not with the chick or mother inbreeding effects on offspring tarsus (Fig. 5, Table S7). As males do not tend nests, this could mean that the male inbreeding by maximum temperature interaction is in fact interaction only with the laying date. Finally, the positive chick inbreeding by temperature and by rainfall interaction effects on SMI were very weak and had the same sign and strength. It is possible that both have the same explanation, for example that in lower temperatures (which often coincide with low rainfall in central Europe) it is slightly more costly for more inbred chicks to compensate for loss of energy than it is for more outbred chicks.

Few studies have explored effects of within-pair (i.e. corresponding to the nestling inbreeding coefficient in our study) and parental inbreeding on chick growth and condition. In the collared flycatcher (*Ficedula albicollis*), first-kin inbred fledglings had on average smaller tarsi compared to first-kin outbred fledglings, with a decrease by 0.6 standard deviation in tarsus length, but no inbreeding depression on fledgling body condition was found (Kruuk *et al.* 2002). In the great tit, fledgling body mass (which is correlated with the body size and condition) was unrelated to the inbreeding of the mother or the father (Szulkin *et al.* 2007). In the Leach's storm-petrel, neither nestling nor parental inbreeding were associated with the skeletal body size and body mass growth rate, however, on day 10 post-hatch these metrics were strongly negatively associated with maternal inbreeding (Sin *et al.* 2021).

We conclude that 1) it is parental inbreeding rate, in contrast with the offspring inbreeding rate, that is negatively related to nestling skeletal body size, 2) this relationship is absent in the youngest chicks becomes negative on days 5 and 9 post-hatch, 3) this relationship is more negative for the father inbreeding compared to the mother and chick inbreeding, 4) weather variables and laying date interact with inbreeding depression on chick tarsus and condition, and 5) the parental and offspring inbreeding relationships with the offspring's body size and SMI are weak at the nestling stage.

Conclusions and conservation implications

Our goal was to evaluate inbreeding depression in the aquatic warbler and determine whether inbreeding depression in this species is dependent on phenotypic individual quality-related traits and environmental variables. The aquatic warbler represents a non-model species for which it is difficult to establish within-pair relatedness – because there is no pair bond, and complete father-to-offspring assignment requires high effort to capture males over a large area. Return rates of first-year birds are challenging to study because of their low natal site fidelity, resulting most probably from high juvenile mortality during the first winter migration and potentially also high post-natal dispersal of young (Kubacka *et al.* 2023). It is also challenging to precisely track yearly survival rate of females, which show lower annual return rates compared to males (Bellebaum 2018). As a result, in our study we were not able to assess the cumulative effect of inbreeding over a continuum of life-history traits (Szulkin *et al.* 2007, Grueber *et al.* 2010). Our estimates of the strength of inbreeding depression in the aquatic warbler could therefore be underestimated. In future studies, it would be valuable to address the inbreeding depression on the missing short-term fitness components, e.g. survival from viable egg to sexual maturity, female long-term survival and the lifetime reproductive success. Overall, our study highlights the high effort required, and the methodology difficulties that

need to be overcome to comprehensively determine the strength of inbreeding depression in a non-model species of high conservation concern.

In spite of these challenges, we were able to demonstrate conditional inbreeding depression in the aquatic warbler on some fitness components and fitness-related traits, suggesting that in smaller-bodied individuals – especially males – inbreeding depression can be strong, and that it can act on nestling chick body size and condition only at older age or under certain environmental conditions. Importantly, our results suggest that effects of inbreeding could carry over to the next generation. If due the negative parental inbreeding effects nestlings grow smaller compared to nestlings of more outbred parents, this could compromise their survival to maturity and reproductive success in adulthood, as found in our study for clutch sizes and fledged brood sizes, as well as in some other bird species (Sedinger *et al.* 1995, Gebhardt-Henrich & Richner 1998, Ringsby *et al.* 1998, Seress *et al.* 2020). Finally, our results point out that inbreeding depression in the aquatic warbler could affect extinction risk and therefore highlight the need to carry out a population viability analysis for this species, taking into account effects of inbreeding depression (O'Grady *et al.* 2006, Nonaka *et al.* 2019). This will enable to obtain more precise estimates of extinction risk in a population, and to undertake conservation actions for the aquatic warbler, such as translocation, habitat management or creating stepping-stone habitats in a more informed, cost-efficient and effective way.

Acknowledgements

We are grateful for the field assistance of Grzegorz Kiljan, Pedro Costa, Piotr Guzik, Marta Celej, Julien Foucher, Beata Głębocka, Aneta Gołębiewska, Maciej Kamiński, Agnieszka Kuczyńska, Romuald Mikusek, Łukasz Mucha, Felix Närmann, Edyta Podmokła, Aneta Rybińska, Paulina Siejka, Michał Walesiak, Laura Zani. Gugny Field Station of the Institute of Biology, University of Białystok, Poland kindly provided accommodation and workspace during fieldwork. Susan Mbedi, Ismael Reyes and Katarzyna Dudek supported the preparation and sequencing of RAD libraries. Wiesław Babik provided lab space and equipment for molecular analyses. The labwork and bioinformatic analysis was partially funded by the German Federal Ministry of Education and Research (BMBF, Förderkennzeichen 033W034A). The sequencing was performed in cooperation with the Competence Center for Genome Analysis at the Christian-Albrechts-University in Kiel and at the Berlin Center for Genomics in Biodiversity Research. The study was funded by the Polish National Science Centre's grant no. 2016/20/S/NZ8/00434 awarded to Justyna Kubacka.

References

Alatalo, R. V & Lundberg, A. 1986. HERITABILITY AND SELECTION ON TARSUS LENGTH IN THE PIED FLYCATCHER (FICEDULA HYPOLEUCA). *Evolution* **40**: 574–583.

Andrew, S.C., Hurley, L.L., Mariette, M.M. & Griffith, S.C. 2017. Higher temperatures during development reduce body size in the zebra finch in the laboratory and in the wild. *J. Evol. Biol.* **30**: 2156–2164.

Andrews, K.R., Adams, J.R., Cassirer, E.F., Plowright, R.K., Gardner, C., Dwire, M., Hohenlohe, P.A. & Waits, L.P. 2018. A bioinformatic pipeline for identifying informative SNP panels for parentage assignment from RADseq data. *Mol. Ecol. Resour.* **18**: 1263–1281.

Armbruster, P. & Reed, D.H. 2005. Inbreeding depression in benign and stressful environments. *Heredity* **95**: 235–242.

Bartoń, K. 2019. MuMIn: Multi-Model Inference. R package version 1.43.6.

Bates, D., Mächler, M., Bolker, B. & Walker, S. 2015. Fitting linear mixed-effects models using lme4. *J. Stat. Softw.* **67**: 1–48.

Bayona-Vásquez, N.J., Glenn, T.C., Kieran, T.J., Pierson, T.W., Hoffberg, S.L., Scott, P.A., Bentley, K.E., Finger, J.W., Louha, S., Troendle, N., Diaz-Jaimes, P., Mauricio, R. & Faircloth, B.C. 2019. Adapterama III: Quadruple-indexed, double/triple-enzyme RADseq libraries (2RAD/3RAD). *PeerJ* **7**: e7724.

Bellebaum, J. 2018. Population dynamics. In: *The Aquatic Warbler conservation handbook* (F. Tanneberger & J. Kubacka, eds), pp. 68–71. Brandenburg State Office for Environment (LfU), Potsdam, Germany.

Blasco-Moreno, A., Pérez-Casany, M., Puig, P., Morante, M. & Castells, E. 2019. What does a zero mean? Understanding false, random and structural zeros in ecology. *Methods Ecol. Evol.* **10**: 949–959.

Bolger, A.M., Lohse, M. & Usadel, B. 2014. Trimmomatic: a flexible trimmer for Illumina sequence data. *Bioinformatics* **30**: 2114–2120.

Brook, B.W., Tonkyn, D.W., O'Grady, J.J. & Frankham, R. 2002. Contribution of inbreeding to extinction risk in threatened species. *Ecol. Soc.* **6**: 16.

Brown, C.R. & Brown, M.B. 2003. Testis size increases with colony size in cliff swallows. *Behav. Ecol.* **14**: 569–575.

Burnham, K.P. & Anderson, D.R. 2002. *Model Selection and Multimodel Inference: A Practical Information-Theoretic Approach*, 2nd ed. Springer-Verlag, New York, USA.

Campbell, H. 2021. The consequences of checking for zero-inflation and overdispersion in the analysis of count data. *Methods Ecol. Evol.* **12**: 665–680.

Canty, A. & Ripley, B.D. 2021. boot: Bootstrap R (S-Plus) Functions.

Catchen, J., Hohenlohe, P.A., Bassham, S., Amores, A. & Cresko, W.A. 2013. Stacks: An analysis tool set for population genomics. *Mol. Ecol.* **22**: 3124–3140.

Catchen, J.M., Amores, A., Hohenlohe, P., Cresko, W. & Postlethwait, J.H. 2011. Stacks: Building and Genotyping Loci De Novo From Short-Read Sequences. *G3 Genes|Genomes|Genetics* **1**: 171–182.

Chapman, J.R., Nakagawa, S., Coltman, D.W., Slate, J. & Sheldon, B.C. 2009. A quantitative review of heterozygosity–fitness correlations in animal populations. *Mol. Ecol.* **18**: 2746–2765.

Cleasby, I.R., Burke, T., Schroeder, J. & Nakagawa, S. 2011. Food supplements increase adult tarsus

length, but not growth rate, in an island population of house sparrows (Passer domesticus). *BMC Res. Notes* **4**: 431.

Crnokrak, P. & Roff, D.A. 1999. Inbreeding depression in the wild. *Heredity* **83**: 260–270.

Danecek, P., Auton, A., Abecasis, G., Albers, C.A., Banks, E., DePristo, M.A., Handsaker, R.E., Lunter, G., Marth, G.T., Sherry, S.T., McVean, G., Durbin, R. & Group, 1000 Genomes Project Analysis. 2011. The variant call format and VCFtools. *Bioinformatics* **27**: 2156–2158.

David, P., Pujol, B., Viard, F., Castella, V. & Goudet, J. 2007. Reliable selfing rate estimates from imperfect population genetic data. *Mol. Ecol.* **16**: 2474–2487.

Davison, A.C. & Hinkley, D. V. 1997. *Bootstrap Methods and Their Applications*. Cambridge University Press, Cambridge.

De Kogel, C.H. 1997. Long-Term Effects of Brood Size Manipulation on Morphological Development and Sex-Specific Mortality of Offspring. *J. Anim. Ecol.* **66**: 167–178.

Dhondt, A.A. 1982. HERITABILITY OF BLUE TIT TARSUS LENGTH FROM NORMAL AND CROSS-FOSTERED BROODS. *Evolution* **36**: 418–419.

Dodt, M., Roehr, J.T., Ahmed, R. & Dieterich, C. 2012. FLEXBAR-Flexible Barcode and Adapter Processing for Next-Generation Sequencing Platforms. *Biology (Basel).* **1**: 895–905.

Driller, M., Arantes, L.S., Vilaça, S.T., Carrasco-Valenzuela, T., Heeger, F., Mbedi, S., Chevallier, D., De Thoisy, B. & Mazzoni, C.J. 2021. Achieving high-quality ddRAD-like reference catalogs for non-model species: the power of overlapping paired-end reads. *bioRxiv* 2020.04.03.024331.

Dyrcz, A. 1993. Nesting biology of the Aquatic Warbler (Acrocephalus paludicola) in the Biebrza Marshes (NE Poland). *Vogelwelt* **114**: 2–15.

Dyrcz, A., Wink, M., Kruszewicz, A. & Leisler, B. 2005. Male reproductive success is correlated with blood parasite levels and body condition in the promiscuous Aquatic Warbler (*Acrocephalus paludicola*). *Auk* **122**: 558–565.

Dyrcz, A. & Zdunek, W. 1993a. Breeding ecology of the Aquatic Warbler *Acrocephalus paludicola* on the Biebrza marshes, northeast Poland. *Ibis* **135**: 181–189.

Dyrcz, A. & Zdunek, W. 1993b. Breeding statistics of the Aquatic WarblerAcrocephalus paludicola on the Biebrza marshes, northeast Poland. *J. Ornithol.* **134**: 317–323.

Evans, S.R. & Sheldon, B.C. 2008. Interspecific patterns of genetic diversity in birds: correlations with extinction risk. *Conserv. Biol.* **22**: 1016–1025.

Faux, P., Oliveira, J.C.P., Campos, D.P., Dantas, G.P.M., Maia, T.A., Dergan, C.G., Cassemiro, P.M., Hajdu, G.L., Santos-Júnior, J.E. & Santos, F.R. 2020. Fast genomic analysis of aquatic bird populations from short single-end reads considering sex-related pitfalls. *Ecol. Inform.* **56**: 101058.

Flade, M., Malashevich, U., Krogulec, J., Poluda, A., Preiksa, Z., Végvári, Z. & Lachmann, L. 2018. World distribution, population, and trends. In: *The Aquatic Warbler conservation handbook* (F. Tanneberger & J. Kubacka, eds), pp. 22–35. Brandenburg State Office for Environment (LfU), Potsdam, Germany.

Flanagan, S.P. & Jones, A.G. 2019. The future of parentage analysis: From microsatellites to SNPs and beyond. *Mol. Ecol.* **28**: 544–567.

Forstmeier, W., Ihle, M., Opatová, P., Martin, K., Knief, U., Albrechtová, J., Albrecht, T. & Kempenaers, B. 2017. Testing the phenotype-linked fertility hypothesis in the presence and absence of inbreeding. *J. Evol. Biol.* **30**: 968–976.

Fox, C.W. & Reed, D. 2010. Inbreeding depression increases with maternal age in a seed-feeding

beetle. *Evol. Ecol. Res.* **12**: 961–972.

Gage, M.J.G., Surridge, A.K., Tomkins, J.L., Green, E., Wiskin, L., Bell, D.J. & Hewitt, G.M. 2006. Reduced heterozygosity depresses sperm quality in wild rabbits, Oryctolagus cuniculus. *Curr. Biol.* **16**: 612–617.

Garamszegi, L.Z., Török, J., Tóth, L. & Michl, G. 2004. Effect of timing and female quality on clutch size in the Collared Flycatcher Ficedula albicollis . *Bird Study* **51**: 270–277.

Gebhardt-Henrich, S. & Richner, H. 1998. Causes of Growth Variation and Its Consequences for Fitness.

Glenn, T.C., Nilsen, R.A., Kieran, T.J., Sanders, J.G., Bayona-Vásquez, N.J., Finger, J.W., Pierson, T.W., Bentley, K.E., Hoffberg, S.L., Louha, S., Garcia-De Leon, F.J., Del Rio Portilla, M.A., Reed, K.D., Anderson, J.L., Meece, J.K., Aggrey, S.E., Rekaya, R., Alabady, M., Belanger, M., Winker, K. & Faircloth, B.C. 2019. Adapterama I: universal stubs and primers for 384 unique dual-indexed or 147,456 combinatorially-indexed Illumina libraries (iTru & iNext). *PeerJ* **7**: e7755.

Green, J.A. 2021. Too many zeros and/or highly skewed? A tutorial on modelling health behaviour as count data with Poisson and negative binomial regression. *Heal. Psychol. Behav. Med.* **9**: 436–455.

Grueber, C.E., Laws, R.J., Nakagawa, S. & Jamieson, I.G. 2010. Inbreeding depression accumulation across life-history stages of the endangered takahe. *Conserv. Biol.* **24**: 1617–1625.

Grueber, C.E., Nakagawa, S., Laws, R.J. & Jamieson, I.G. 2011. Multimodel inference in ecology and evolution: challenges and solutions. *J. Evol. Biol.* **24**: 699–711.

Harrell, F.E. 2015. Multivariable Modeling Strategies BT - Regression Modeling Strategies: With Applications to Linear Models, Logistic and Ordinal Regression, and Survival Analysis. In: (J. Harrell Frank E., ed), pp. 63–102. Springer International Publishing, Cham.

Harrisson, K.A., Magrath, M.J.L., Yen, J.D.L., Pavlova, A., Murray, N., Quin, B., Menkhorst, P., Miller, K.A., Cartwright, K. & Sunnucks, P. 2019. Lifetime Fitness Costs of Inbreeding and Being Inbred in a Critically Endangered Bird. *Curr. Biol.* **29**: 2711-2717.e4.

Hayward, A. & Gillooly, J.F. 2011. The Cost of Sex: Quantifying Energetic Investment in Gamete Production by Males and Females. *PLoS One* **6**: e16557.

Hemmings, N., West, M. & Birkhead, T.R. 2012a. Causes of hatching failure in endangered birds. *Biol. Lett.* **8**: 964–967.

Hemmings, N.L., Slate, J. & Birkhead, T.R. 2012b. Inbreeding causes early death in a passerine bird. *Nat. Commun.* **3**: 863.

Hinkson, K.M. & Poo, S. 2020. Inbreeding depression in sperm quality in a critically endangered amphibian. *Zoo Biol.* **39**: 197–204.

Huisman, J. 2017. Pedigree reconstruction from SNP data: parentage assignment, sibship clustering and beyond. *Mol. Ecol. Resour.* **17**: 1009–1024.

Huisman, J., Kruuk, L.E.B., Ellis, P.A., Clutton-Brock, T. & Pemberton, J.M. 2016. Inbreeding depression across the lifespan in a wild mammal population. *Proc. Natl. Acad. Sci.* **113**: 3585–3590.

Jamieson, I.G., Roy, M.S. & Lettink, M. 2003. Sex-Specific Consequences of Recent Inbreeding in an Ancestrally Inbred Population of New Zealand Takahe. *Conserv. Biol.* **17**: 708–716.

Kalinowski, S.T., Taper, M.L. & Marshall, T.C. 2007. Revising how the computer program cervus accommodates genotyping error increases success in paternity assignment. *Mol. Ecol.* **16**: 1099–1106.

Kardos, M., Luikart, G. & Allendorf, F.W. 2015. Measuring individual inbreeding in the age of genomics: marker-based measures are better than pedigrees. *Heredity* **115**: 63–72.

Keller, L.F. 1998. Inbreeding and Its Fitness Effects in an Insular Population of Song Sparrows (Melospiza melodia). *Evolution* **52**: 240–250.

Keller, L.F., Grant, P.R., Grant, B.R. & Petren, K. 2002. Environmental conditions affect the magnitude of inbreeding depression in survival of Darwin's finches. *Evolution* **56**: 1229–1239.

Keller, L.F. & Waller, D.M. 2002. Inbreeding effects in wild populations. *Trends Ecol. Evol.* **17**: 230–241.

Kennedy, E.S., Grueber, C.E., Duncan, R.P. & Jamieson, I.G. 2014. SEVERE INBREEDING DEPRESSION AND NO EVIDENCE OF PURGING IN AN EXTREMELY INBRED WILD SPECIES—THE CHATHAM ISLAND BLACK ROBIN. *Evolution* **68**: 987–995.

Kruuk, L.E.B., Merilä, J. & Sheldon, B.C. 2001. Phenotypic Selection on a Heritable Size Trait Revisited. *Am. Nat.* **158**: 557–571.

Kruuk, L.E.B., Sheldon, B.C. & Merilä, J. 2002. Severe inbreeding depression in collared flycatchers (Ficedula albicollis). *Proceedings. Biol. Sci.* **269**: 1581–1589.

Kubacka, J., Dubiec, A., Korb, J., Salewski, V., Dyrcz, A., Foucher, J., Giessing, B., Leisler, B., Schulze-Hagen, K., Wink, M. & Panagiotopoulou, H. 2023. Low genetic diversity and high gene flow in the Aquatic Warbler (Acrocephalus paludicola), a threatened marshland songbird with a fragmented breeding range. *Ibis* **n/a**.

Kubacka, J., Oppel, S., Dyrcz, A., Lachmann, L., Barros Da Costa, J.P.D., Kail, U. & Zdunek, W. 2014. Effect of mowing on productivity in the endangered Aquatic Warbler Acrocephalus paludicola. *Bird Conserv. Int.* **24**: 45–58.

Langmead, B., Trapnell, C., Pop, M. & Salzberg, S.L. 2009. Ultrafast and memory-efficient alignment of short DNA sequences to the human genome. *Genome Biol.* **10**: R25.

Le Nevé, A., Blaize, C., Dehorter, O., Dugué, H., Hemery, D., Jiguet, F., Musseau, R., Neto, J.M., Rguibi Idrissi, H., Zumalacárregui Martínez, C. & Roothaert, N. 2018. Migration. In: *The Aquatic Warbler conservation handbook* (F. Tanneberger & J. Kubacka, eds), pp. 72–89. Brandenburg State Office for Environment (LfU), Potsdam, Germany.

Liker, A., Papp, Z., Bókony, V. & Lendvai, Á.Z. 2008. Lean birds in the city: body size and condition of house sparrows along the urbanization gradient. *J. Anim. Ecol.* **77**: 789–795.

Martin, M. 2011. Cutadapt removes adapter sequences from high-throughput sequencing reads. *EMBnet.journal; Vol 17, No 1 Next Gener. Seq. Data Anal.*, doi: 10.14806/ej.17.1.200.

Matthews, T.J., Cottee-Jones, H.E. & Whittaker, R.J. 2014. Habitat fragmentation and the species–area relationship: a focus on total species richness obscures the impact of habitat loss on habitat specialists. *Divers. Distrib.* **20**: 1136–1146.

Mazerolle, M.J. 2019. AICcmodavg: Model selection and multimodel inference based on (Q)AIC(c). R package version 2.2-2.

Mazerolle, M.J. 2023. AICcmodavg: Model selection and multimodel inference based on (Q)AIC(c).

Merilä, J. & Fry, J.D. 1998. Genetic Variation and Causes of Genotype-Environment Interaction in the Body Size of Blue Tit (Parus caeruleus). *Genetics* **148**: 1233–1244.

Morton, N.E. & Crow, J.F. 1956. An Estimate of the Mutational Damage in Man from Data on Consanguineous Marriages. *Proc. Natl. Acad. Sci. U. S. A.* **42**: 855–863.

Nietlisbach, P., Muff, S., Reid, J.M., Whitlock, M.C. & Keller, L.F. 2019. Nonequivalent lethal equivalents: Models and inbreeding metrics for unbiased estimation of inbreeding load. *Evol.*

Appl. **12**: 266–279.

Nip, E.J., Frei, B. & Elliott, K.H. 2018. Seasonal and temporal variation in scaled mass index of Black-capped Chickadees (*Poecile atricapillus*). *Can. F. Nat.* **132**: 368–377.

Niskanen, A.K., Billing, A.M., Holand, H., Hagen, I.J., Araya-Ajoy, Y.G., Husby, A., Rønning, B., Myhre, A.M., Ranke, P.S., Kvalnes, T., Pärn, H., Ringsby, T.H., Lien, S., Sæther, B.-E., Muff, S. & Jensen, H. 2020. Consistent scaling of inbreeding depression in space and time in a house sparrow metapopulation. *Proc. Natl. Acad. Sci.* **117**: 14584–14592.

Nonaka, E., Sirén, J., Somervuo, P., Ruokolainen, L., Ovaskainen, O. & Hanski, I. 2019. Scaling up the effects of inbreeding depression from individuals to metapopulations. *J. Anim. Ecol.* **88**: 1202–1214.

Noordwijk, A.J. Van, Balen, J.H. Van & Scharloo, W. 1988. Heritability of body size in a natural population of the Great Tit (Parus major) and its relation to age and environmental conditions during growth. *Genet. Res.* **51**: 149–162.

Noordwijk, A.J. Van & Scharloo, W. 1981. Inbreeding in an Island Population of the Great Tit. *Evolution* **35**: 674–688.

Nowak, C., Jost, D., Vogt, C., Oetken, M., Schwenk, K. & Oehlmann, J. 2007. Consequences of inbreeding and reduced genetic variation on tolerance to cadmium stress in the midge Chironomus riparius. *Aquat. Toxicol.* **85**: 278–284.

O'Grady, J.J., Brook, B.W., Reed, D.H., Ballou, J.D., Tonkyn, D.W. & Frankham, R. 2006. Realistic levels of inbreeding depression strongly affect extinction risk in wild populations. *Biol. Conserv.* **133**: 42–51.

Parker, G.A. & Pizzari, T. 2010. Sperm competition and ejaculate economics. *Biol. Rev.* **85**: 897–934.

Peig, J. & Green, A.J. 2009. New perspectives for estimating body condition from mass/length data: the scaled mass index as an alternative method. *Oikos* **118**: 1883–1891.

Pflüger, F.J., Signer, J. & Balkenhol, N. 2019. Habitat loss causes non-linear genetic erosion in specialist species. *Glob. Ecol. Conserv.* **17**: e00507.

Potti, J. & Merino, S. 1994. Heritability estimates and maternal effects on tarsus length in pied flycatchers, Ficedula hypoleuca. *Oecologia* **100**: 331–338.

Puig, P. & Valero, J. 2006. Count Data Distributions: Some Characterizations with Applications. *J. Am. Stat. Assoc.* **101**: 332–340.

R Core Team. 2023. R: A Language and Environment for Statistical Computing.

Ralls, K., Ballou, J.D. & Templeton, A. 1988. Estimates of Lethal Equivalents and the Cost of Inbreeding in Mammals. *Conserv. Biol.* **2**: 185–193.

Ringsby, T.H., Saether, B.-E. & Solberg, E.J. 1998. Factors affecting juvenile survival in house sparrow *Passer domesticus*. *J. Avian Biol.* **29**: 241–247.

Rising, J.D. & Somers, K.M. 1989. The Measurement of Overall Body Size in Birds. *Auk* **106**: 666–674.

Rochette, N.C. & Catchen, J.M. 2017. Deriving genotypes from RAD-seq short-read data using Stacks. *Nat. Protoc.* **12**: 2640–2659.

Scholer, M.N., Strimas-Mackey, M. & Jankowski, J.E. 2020. A meta-analysis of global avian survival across species and latitude. *Ecol. Lett.* **23**: 1537–1549.

Schulze-Hagen, K., Flinks, H. & Dyrcz, A. 1989. Brutzeitliche Beutewahl beim Seggenrohrsänger *Acrocephalus paludicola*. *J. Ornithol.* **130**: 251–255.

Searcy, W.A., Peters, S. & Nowicki, S. 2004. Effects of early nutrition on growth rate and adult size in

song sparrows Melospiza melodia. *J. Avian Biol.* **35**: 269–279.

Sedinger, J.S., Flint, P.L. & Lindberg, M.S. 1995. Environmental Influence on Life-History Traits: Growth, Survival, and Fecundity in Black Brant (Branta Bernicla). *Ecology* **76**: 2404–2414.

Senar, J.C. & Pascual, J. 1997. Keel and tarsus length may provide a good predictor of avian body size. *Ardea* **85**.

Seress, G., Sándor, K., Evans, K.L. & Liker, A. 2020. Food availability limits avian reproduction in the city: An experimental study on great tits Parus major. *J. Anim. Ecol.* **89**: 1570–1580.

Sin, S.Y.W., Hoover, B.A., Nevitt, G.A. & Edwards, S. V. 2021. Demographic History, Not Mating System, Explains Signatures of Inbreeding and Inbreeding Depression in a Large Outbred Population. *Am. Nat.* **197**: 658–676.

Smith, J.N.M. & Dhondt, A.A. 1980. Experimental Confirmation of Heritable Morphological Variation in a Natural Population of Song Sparrows. *Evolution* **34**: 1155–1158.

Stoffel, M.A., Esser, M., Kardos, M., Humble, E., Nichols, H., David, P. & Hoffman, J.I. 2016. inbreedR: an R package for the analysis of inbreeding based on genetic markers. *Methods Ecol. Evol.* **7**: 1331–1339.

Symonds, M.R.E. & Moussalli, A. 2011. A brief guide to model selection, multimodel inference and model averaging in behavioural ecology using Akaike's information criterion. *Behav. Ecol. Sociobiol.* **65**: 13–21.

Szulkin, M., Bierne, N. & David, P. 2010. Heterozygosity-fitness correlations: a time for reappraisal. *Evolution* **64**: 1202–1217.

Szulkin, M., Garant, D., McCleery, R.H. & Sheldon, B.C. 2007. Inbreeding depression along a life-history continuum in the great tit. *J. Evol. Biol.* **20**: 1531–1543.

Szulkin, M. & Sheldon, B.C. 2007. The Environmental Dependence of Inbreeding Depression in a Wild Bird Population. *PLoS One* **2**: e1027.

Tanneberger, F., Alexander, K., Poluda, A., Bellebaum, J., Lachmann, L. & Flade, M. 2018a. Threats and limiting factors. In: *The Aquatic Warbler conservation handbook* (F. Tanneberger & J. Kubacka, eds), pp. 106–121. Brandenburg State Office for Environment (LfU), Potsdam, Germany.

Tanneberger, F., Kloskowski, J., Knöfler, V., Kozulin, A., Marczakiewicz, Piotr Morkvėnas, Ž., Poluda, A., Végvári, Z., Vergeichik, L. & Flade, M. 2018b. Breeding habitat requirements. In: *The Aquatic Warbler conservation handbook* (F. Tanneberger & J. Kubacka, eds), pp. 34–45. Brandenburg State Office for Environment (LfU), Potsdam, Germany.

Thrasher, D.J., Butcher, B.G., Campagna, L., Webster, M.S. & Lovette, I.J. 2018. Double-digest RAD sequencing outperforms microsatellite loci at assigning paternity and estimating relatedness: A proof of concept in a highly promiscuous bird. *Mol. Ecol. Resour.* **18**: 953– 965.

Venables, W.N. & Ripley, B.D. 2002. *Modern Applied Statistics with S*, Fourth. Springer, New York.

Vitorino, L.C., Borges Souza, U.J., Jardim, T.P.F.A. & Ballesteros–mejia, L. 2019. Towards inclusion of genetic diversity measures into IUCN assessments: a case study on birds. *Anim. Biodivers. Conserv.* **42.2**: 317–335.

Wang, J. 2014. Marker-based estimates of relatedness and inbreeding coefficients: an assessment of current methods. *J. Evol. Biol.* **27**: 518–530.

Westemeier, R.L., Brawn, J.D., Simpson, S.A., Esker, T.L., Jansen, R.W., Walk, J.W., Kershner, E.L., Bouzat, J.L. & Paige, K.N. 1998. Tracking the long-term decline and recovery of an isolated population. *Science* **282**: 1695–1698.

Wickham, H. 2016. *ggplot2: Elegant Graphics for Data Analysis*. Springer-Verlag New York.

Wigginton, J.E., Cutler, D.J. & Abecasis, G.R. 2005. A Note on Exact Tests of Hardy-Weinberg Equilibrium. *Am. J. Hum. Genet.* **76**: 887–893.

Wilson, A.J., Pemberton, J.M., Pilkington, J.G., Coltman, D.W., Mifsud, D. V, Clutton-Brock, T.H. & Kruuk, L.E.B. 2006. Environmental Coupling of Selection and Heritability Limits Evolution. *PLOS Biol.* **4**: e216.

Zeileis, A. & Kleiber, C. 2022. {countreg}: Count Data Regression.

Zeileis, A., Kleiber, C. & Jackman, S. 2008. Regression Models for Count Data in {R}. *J. Stat. Softw.* **27**: 1–25.

Zhang, J., Kobert, K., Flouri, T. & Stamatakis, A. 2014. PEAR: a fast and accurate Illumina Paired-End reAd mergeR. *Bioinformatics* **30**: 614–620.

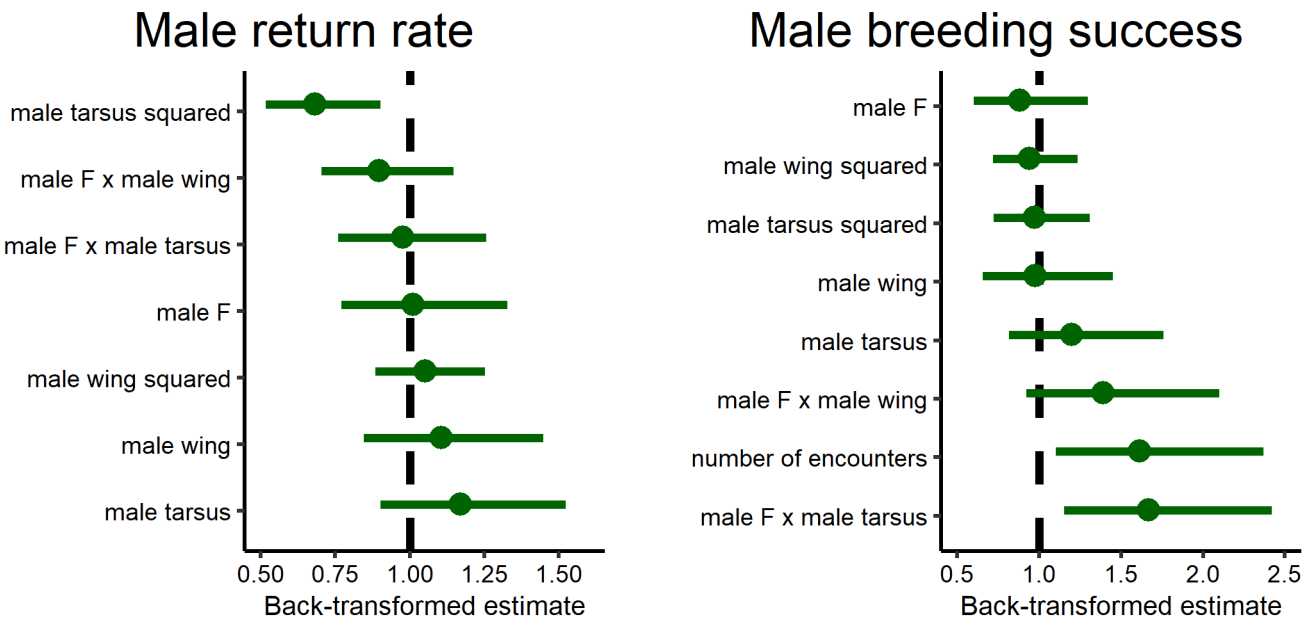

Fig. 1 Estimates (denoted by circles) of effects of the male inbreeding coefficient *F*, phenotypic variables (tarsus and wing length) and their interaction with *F* on male fitness components: 4-year return rate to breeding grounds (left) and seasonal breeding success (right). The whiskers represent 95% confidence intervals and the vertical dashed line refers to no effect. See Table S3 for the summary of estimates

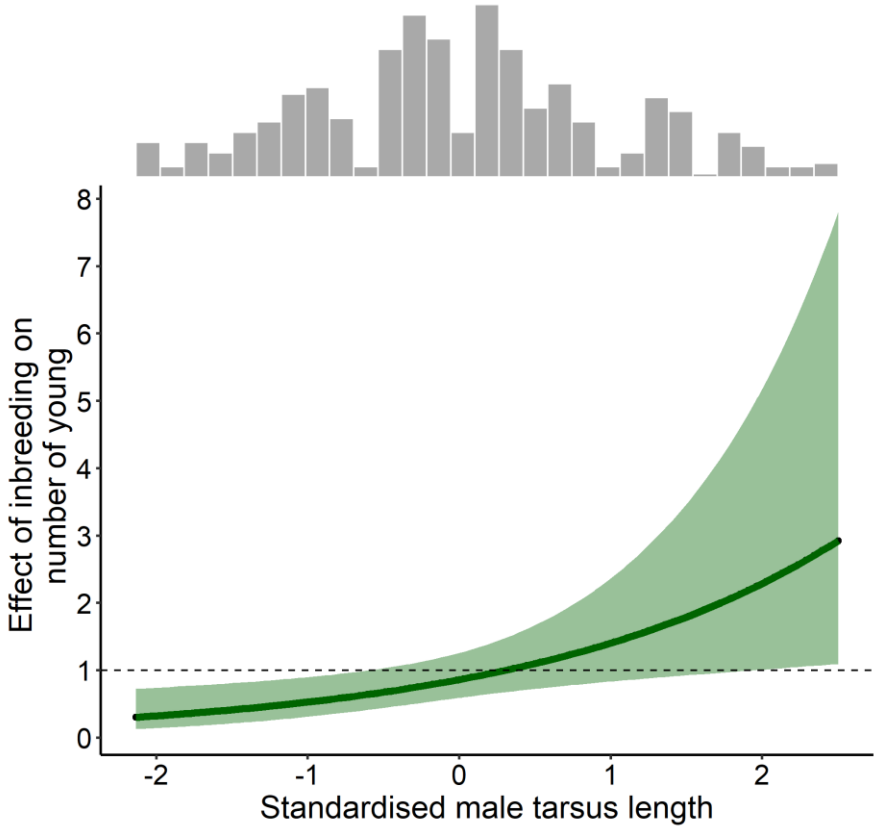

Fig. 2 Interaction between tarsus length and the inbreeding coefficient *F* on male seasonal breeding success. The curve shows the back-transformed statistical effect of inbreeding plotted against tarsus length, and the bands show the confidence interval of the effect. The horizontal dashed line corresponds to no effect. The histogram shows frequency of tarsus lengths

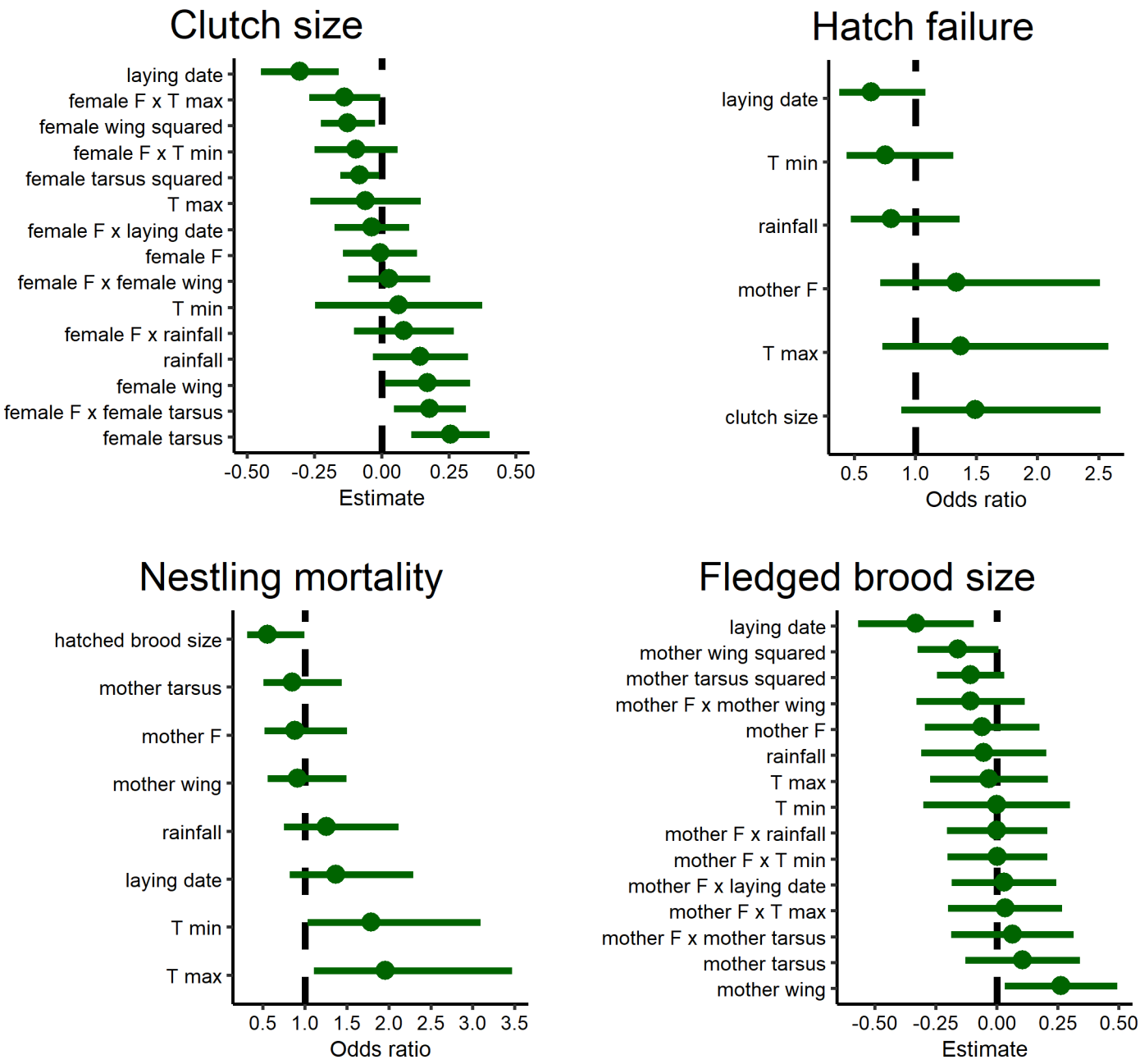

Fig. 3 Estimates (denoted by circles) of effects of the inbreeding coefficient *F*, mother phenotypic variables (tarsus, wing length and laying date), environmental variables (average maximum temperature, average minimum ground temperature and rainfall) and their interaction with *F* on female fitness components: clutch size (top left), hatch failure (top right), nestling mortality from hatching to fledging (bottom left) and fledged brood size in successful nests (bottom right)**.** The whiskers represent 95% confidence intervals and the vertical dashed line refers to no effect. See Table S5 summary of estimates

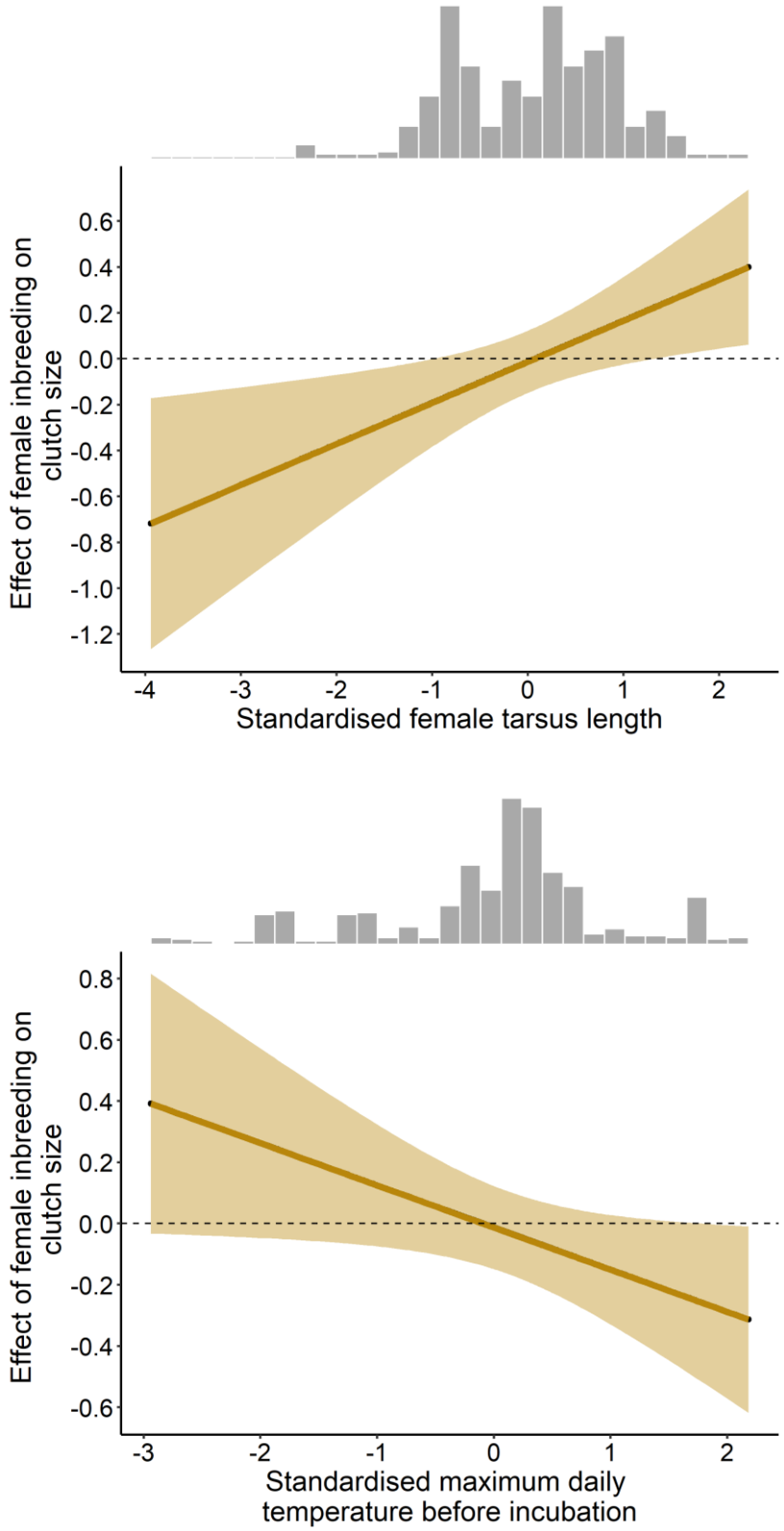

Fig. 4. Interaction of female inbreeding rate with female tarsus length (top) and the average maximum daily temperature during two weeks before the onset of incubation (bottom). The graphs present model fits and illustrate how the statistical effects of the female inbreeding rate change along the value of the modifying variable. The bands show confidence intervals of the effects, the horizontal dashed line corresponds to no effect, and the histogram shows frequency of tarsus lengths (top) and temperatures (bottom)

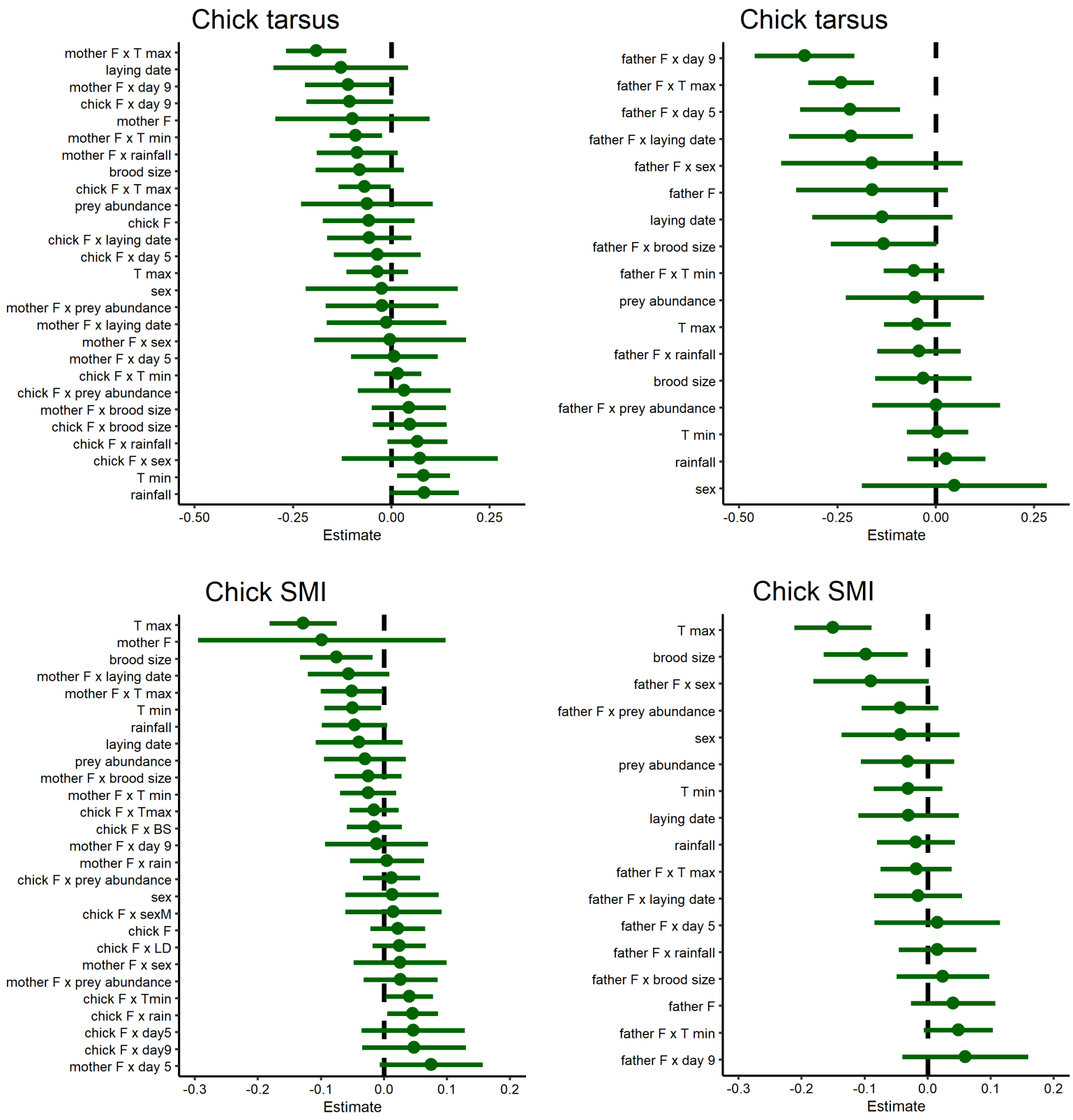

Fig. 5 Estimates (denoted by circles) of effects of the chick and mother inbreeding coefficients *F* (left) and father *F* (right), environmental variables (laying date, brood size, average maximum temperature, average minimum ground temperature, rainfall, brood size and prey abundance) and their interaction with *F* on chick tarsus length (top) and scaled mass index, SMI (bottom) on days 2, 5 and 9 post-hatch. The whiskers represent 95% confidence intervals and the vertical dashed line refers to no effect. See Tables S6 & S7 for the summary of estimates

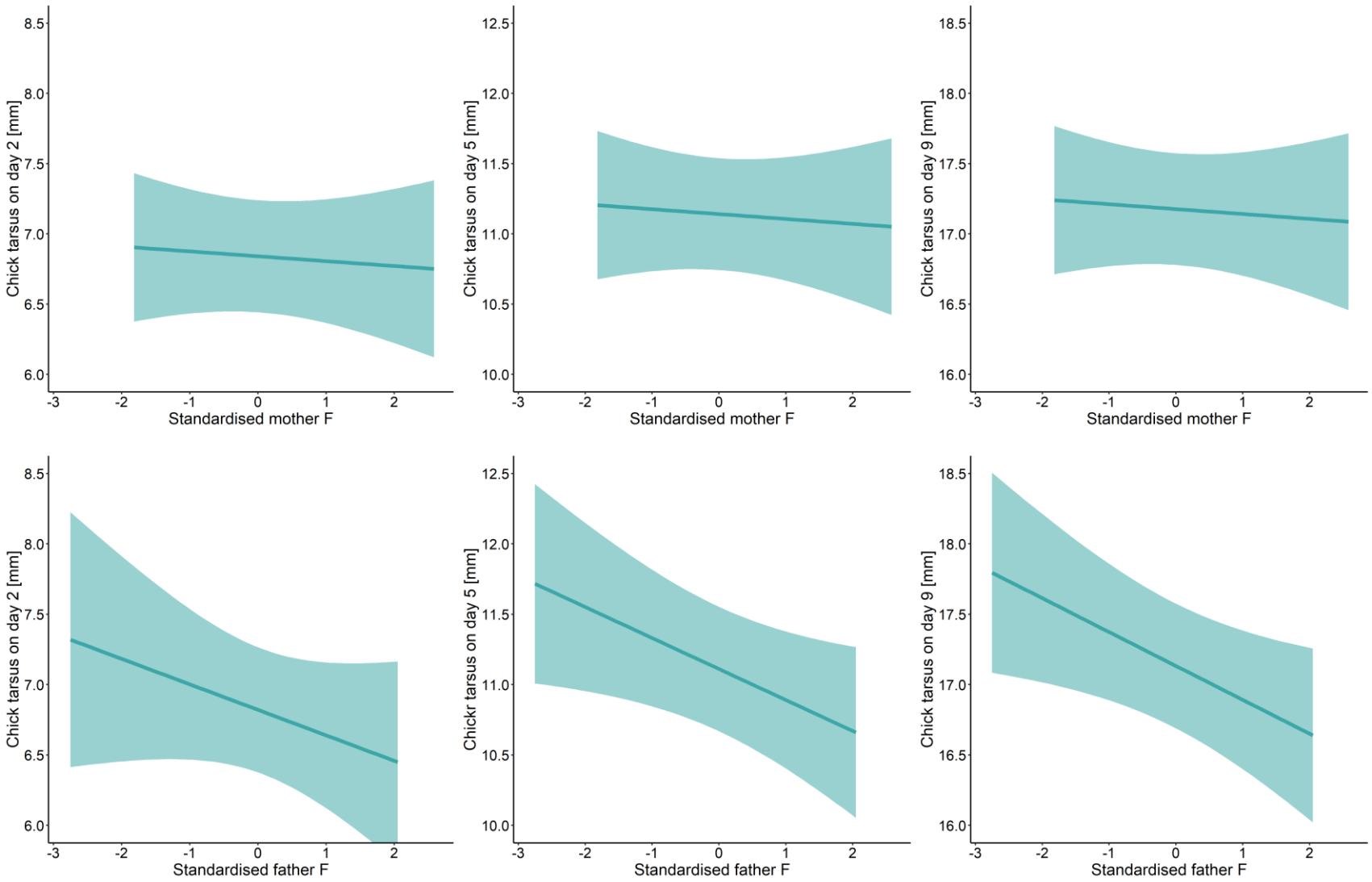

Fig. 6 Mother (top) and father (bottom) inbreeding coefficient *F* relationship with chick tarsus length on days 2, 5 and 9 post-hatch. The curves show fits averaged across models (weighted by ωAICc) and the study areas and years, and the bands show confidence intervals

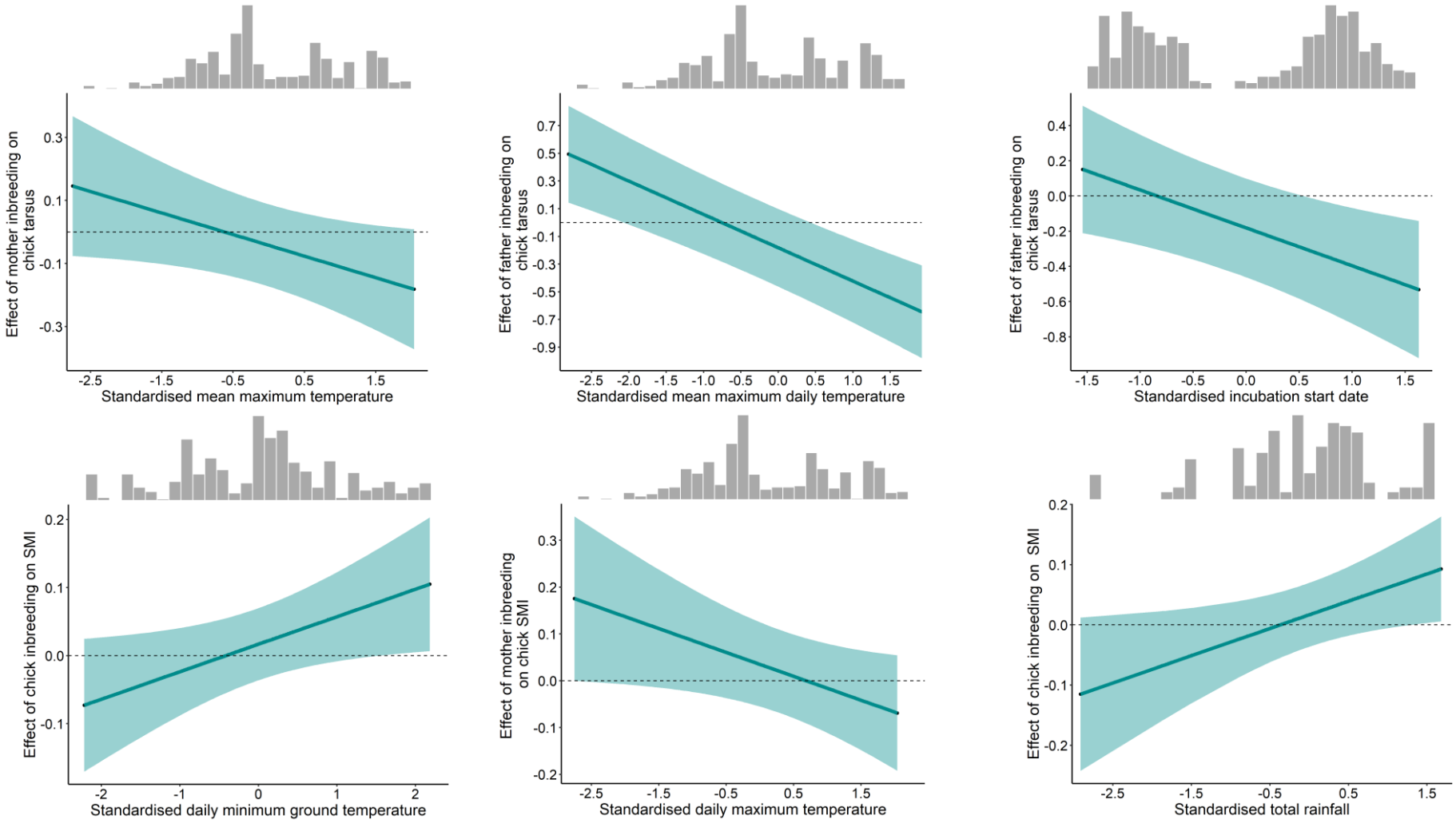

Fig. 7. Interaction effects between parental and chick inbreeding rates and environmental factors on chick tarsus and SMI. The graphs present model fits and illustrate how the statistical effects of the inbreeding rates change along the value of the modifying variables. The bands show confidence intervals of the effects, the horizontal dashed line corresponds to no effect, and the histogram shows frequency of the given environmental factors

Table 1. Inbreeding load (*B*) on the fitness traits and the corresponding inbreeding depression (*δ*) on the fitness and condition components of aquatic warblers. Inbreeding load is expressed in lethal haploid equivalents and was calculated using centred input variables, model-averaged estimates and the log-link. Inbreeding depression is the change in fitness of the most inbred relative to the least inbred individuals in the dataset, and was calculated using model-averaged and back-transformed predictions, averaged for the study areas and years. The variables for which *B* and *δ* are different from zero are marked in bold. CI – confidence interval

Fitness component	Inbreeding determined in:		*B*	95% CI of *B*	Change in trait *δ*
Male long-term survival	male		–0.2[1]	–5.9, 5.5	+2.1%
Male breeding success	male		2.7[1]	–5.6, 11.1	–45.6%
Average small males	male		**11.2[1]**	**9.0, 13.4**	**–75.7%**
Average large males	male		–6.7[1]	–22.9, 8.5	+51.4%
Clutch size	female		0.0	–0.7; 0.7	–1.2%
Average small females	female		**0.7[2]**	**0.6; 0.9**	**–9.5%**
Average large females	female		–0.6[2]	–1.8; 0.6	+6.0%
Hatch failure	female		–0.4[3]	–2.9; 2.1	+25%
Nestling survival to fledging	female		0.5[3]	–2.3; 3.3	–23.0%
Fledged brood size	female		0.4[2]	–1.1; 1.8	–5.7%
Nestling tarsus	nestling	day 2			0.0%
		day 5			0.0%
		day 9			–0.1%
	mother	day 2			–3.1%
		day 5			–2.3%
		day 9			**–2.3%**
	father	day 2			+3.1%
		day 5			**–7.3%**
		day 9			**–7.8%**
Nestling SMI	nestling	day 2			+0.9%
		day 5			+0.6%
		day 9			+0.4%
	mother	day 2			+5.6%
		day 5			+3.2%
		day 9			+1.2%
	father	day 2			+7.5%
		day 5			+3.3%
		day 9			+1.9%

[1] negative binomial distribution used
[2] gaussian distribution used
[3] poisson distribution used